



Thermodynamic linkage between calmodulin domains binding calcium and contiguous sites in the C-terminal tail of Ca_v1.2

T. Idil Apak Evans^{a,1}, Johannes W. Hell^{b,2}, Madeline A. Shea^{a,*}

^a Department of Biochemistry, Roy J. and Lucille A. Carver College of Medicine, University of Iowa, Iowa City, IA 52242-1109, United States

^b Department of Pharmacology, Roy J. and Lucille A. Carver College of Medicine, University of Iowa, Iowa City, IA 52242-1109, United States

ARTICLE INFO

Article history:

Received 20 May 2011

Received in revised form 15 June 2011

Accepted 15 June 2011

Available online 24 June 2011

Keywords:

Allostery

L-type calcium channel

Calmodulin

Calcium

Signal transduction

Gibbs free energy

Thermodynamics

Peptide

Cardiac

Fluorescence anisotropy

Phenylalanine fluorescence

Equilibrium binding

Crystallography

Disorder tendency

Intrinsic disorder

Selectivity

Recognition

Protein–protein interaction

ABSTRACT

Calmodulin (CaM) binding to the intracellular C-terminal tail (CTT) of the cardiac L-type Ca²⁺ channel (Ca_v1.2) regulates Ca²⁺ entry by recognizing sites that contribute to negative feedback mechanisms for channel closing. CaM associates with Ca_v1.2 under low resting [Ca²⁺], but is poised to change conformation and position when intracellular [Ca²⁺] rises. CaM binding Ca²⁺, and the domains of CaM binding the CTT are linked thermodynamic functions. To better understand regulation, we determined the energetics of CaM domains binding to peptides representing pre-IQ sites A₁₅₈₈, and C₁₆₁₄ and the IQ motif studied as overlapping peptides IQ₁₆₄₄ and IQ₁₆₅₀ as well as their effect on calcium binding. (Ca²⁺)₄-CaM bound to all four peptides very favorably ($K_d \leq 2$ nM). Linkage analysis showed that IQ₁₆₄₄–1670 bound with a $K_d \sim 1$ pM. In the pre-IQ region, (Ca²⁺)₂-N-domain bound preferentially to A₁₅₈₈, while (Ca²⁺)₂-C-domain preferred C₁₆₁₄. When bound to C₁₆₁₄, calcium binding in the N-domain affected the tertiary conformation of the C-domain. Based on the thermodynamics, we propose a structural mechanism for calcium-dependent conformational change in which the linker between CTT sites A and C buckles to form an A–C hairpin that is bridged by calcium-saturated CaM.

© 2011 Elsevier B.V. All rights reserved.

Abbreviations: CaM_{1–148}, Full-length mammalian calmodulin, residues 1–148; CaM_{1–80}, N-domain fragment of calmodulin, residues 1–80; CaM_{76–148}, C-domain fragment of calmodulin, residues 76–148; CaMBD, Calmodulin binding domain; Ca_v1.2, Cardiac L-type Ca²⁺-channel type 1.2; CSU, Contacts of structural units; CTT, C-terminal tail; A₁₅₈₈, Synthetic peptide corresponding to residues 1588–1609 of Ca_v1.2 CTT; C₁₆₁₄, Synthetic peptide corresponding to residues 1614–1635 of Ca_v1.2 CTT; IQ₁₆₄₄, Synthetic peptide corresponding to residues 1644–1670 of Ca_v1.2 CTT; IQ₁₆₅₀, Synthetic peptide corresponding to residues 1650–1675 of Ca_v1.2 CTT; EGTA, Ethylene glycol bis(aminoethyl ether)-N,N',N',N'-tetraacetic acid; FI-A₁₅₈₈, xA₁₅₈₈ fluoresceinated at the N-terminus; FI-C₁₆₁₄, C₁₆₁₄ fluoresceinated at the N-terminus; FI-IQ₁₆₄₄, IQ₁₆₄₄ fluoresceinated at the N-terminus; FI-IQ₁₆₅₀, IQ₁₆₅₀ fluoresceinated at the N-terminus; NTA, Nitrilo-triacetic acid; WT, Wild-type.

* Corresponding author. Tel.: +1 319 335 7885; fax: +1 319 335 9570.

E-mail addresses: idil-apak@uiowa.edu (T.I.A. Evans), jwhell@ucdavis.edu (J.W. Hell), madeline-shea@uiowa.edu (M.A. Shea).

¹ Present address: Department of Anatomy and Cell Biology, Roy J. and Lucille A. Carver College of Medicine, University of Iowa, Iowa City, IA, United States.

² Present address: Department of Pharmacology, University of California Davis, Davis, CA, United States.

1. Introduction

CaM is a ubiquitous Ca²⁺ sensor protein with two EF-hand domains, each of which binds two Ca²⁺ ions. The N-domain (Ca²⁺-binding sites I and II) and C-domain (Ca²⁺-binding sites III and IV) are connected by a flexible linker region (Fig. 1A). These domains are highly homologous at the sequence level, yet their affinities for Ca²⁺ differ by an order of magnitude in all eukaryotes. Changes in intracellular calcium are transduced into temporal control of events regulated by the targets of CaM. The separation in ligand-binding energies occurs primarily because of anti-cooperative interactions between the domains mediated by residues in the linker region. It is widely recognized that these thermodynamic differences are physiologically significant. They allow changes in intracellular calcium levels to trigger sequential conformational changes linked to temporal control of physiological events.

CaM binds to and regulates the activity of a variety of target proteins under Ca²⁺-depleted (apo) and Ca²⁺-saturated conditions [1]. Voltage-

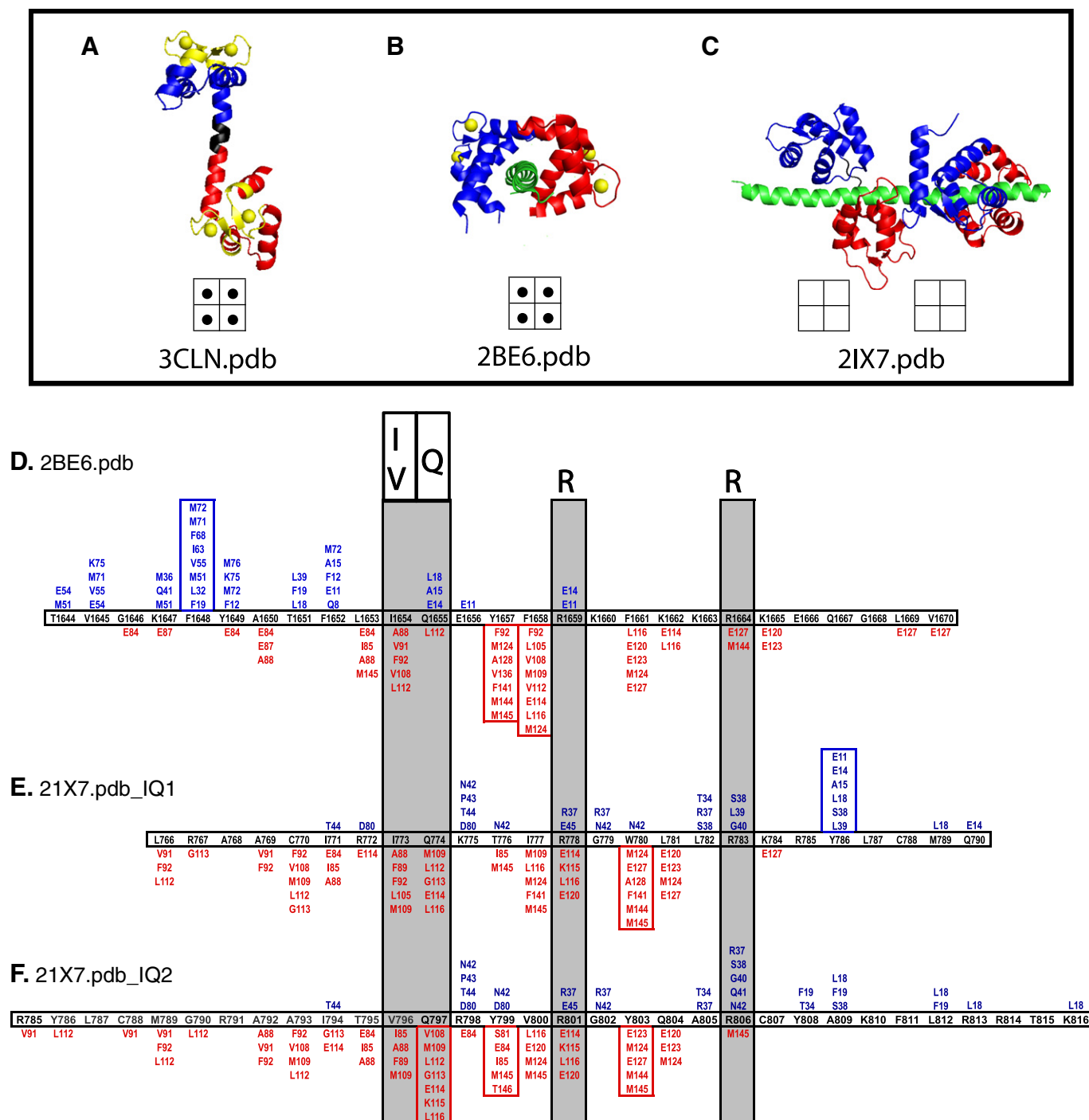


Fig. 1. Ribbon diagrams and contacts of structural units (CSU) analysis of CaM (alone) and in complex with various targets. (A–C) Ribbon diagrams of $(\text{Ca}^{2+})_4\text{-CaM}_{1-148}$ (3CLN.pdb), $(\text{Ca}^{2+})_4\text{-CaM}_{1-148}$ in complex with the IQ-peptide from the C-terminal tail of $\text{Ca}_v1.2$ (2BE6.pdb) and apo CaM in complex with the IQ-peptide from myosin V (21X7.pdb). (D–F) CSU Analysis of CaM in complex with the IQ-peptide from the C-terminal tail of $\text{Ca}_v1.2$ (2BE6.pdb) and the two IQ-motifs of myosin V (21X7.pdb_IQ1 and 21X7.pdb_IQ2). Residues of the N- and C-domains of CaM that are within 4.5 Å of the peptide upon binding are shown in blue and red, respectively. The locations where the greatest number of CaM residues interacts with the peptide are indicated by a box around those CaM residues.

gated Ca^{2+} channels (Ca_v) are oligomeric proteins (α_1 , β , α_2/δ and γ subunits) that contribute to normal heart function by regulating Ca^{2+} entry into the cell. Both the α_1 - and β -subunits of $\text{Ca}_v1.2$ contribute to modulating the activity of the channel upon interacting with other proteins, including Ca^{2+} /calmodulin (CaM) dependent kinase II (CaMKII) [2–5] and CaM [6].

Early studies attributed regulation of activity of the $\text{Ca}_v1.2$ channel to an EF-hand motif located upstream of the $\text{Ca}_v1.2$ CTT [7,8]. However, it is now widely accepted that CaM directly binds to

sites in $\text{Ca}_v1.2$ CTT and regulates its activity in a domain-specific manner (see review articles [9,10]). The C-domain of CaM has been implicated in Ca^{2+} -dependent inactivation (CDI) of $\text{Ca}_v1.2$. It is thought to do so by limiting Ca^{2+} entry through the channel, which is mediated by the local Ca^{2+} -selectivity of the C-domain of CaM [11]. Although the role of the CaM N-domain in regulating $\text{Ca}_v1.2$ was not addressed in the same study [11], another report suggested that the N-domain may also be involved in mediating CDI through local Ca^{2+} -selectivity [12].

Structures of CaM bound to peptides containing IQ motifs showed that each domain of CaM may adopt different conformations depending on the sites occupied by calcium. For example, Ca^{2+} -depleted (apo) CaM binds to two contiguous IQ motifs of myosin V [13,14] (Fig. 1B and C) with its C-domain in the “semi-open” form making the majority of CaM-peptide contacts, and its N-domain in the “closed” conformation making few contacts. In contrast, both the N- and C-domain of Ca^{2+} -saturated CaM bind to the IQ motif of the α_1 -subunit of cardiac L-type Ca^{2+} channel ($\text{Ca}_v1.2$) in the “open” tertiary conformation. Further analysis of these structures using *Contacts of Structural Units* (CSU) [15] indicated that the N-domain interacted with $\text{Ca}_v1.2$ residues outside of the canonical IQ motif (Fig. 1D–F).

Previous studies have identified regions on the $\text{Ca}_v1.2$ CTT that serve as CaM binding sites and thereby act as Ca^{2+} sensors (Fig. 2B) [6,8,16–19]. These CaM binding regions are referred to as A, C, IQ and IQ' (Fig. 2) with residue numbers corresponding to their location on rabbit $\text{Ca}_v1.2$ CTT (accession no. P15381). Electrophysiology studies with a CaM mutant defective in Ca^{2+} binding (CaM1234) demonstrated that CDI was blocked, suggesting that CaM may pre-associate with the channel under Ca^{2+} -depleted (apo) conditions [20]. This so

called “pre-association” of CaM with the IQ-region is regarded as important for fast inactivation of the channel after Ca^{2+} enters the cell [17,18,21,22]. CaM binding to other sites on $\text{Ca}_v1.2$ CTT at various Ca^{2+} concentrations has also been reported. Tsien and co-workers suggested that both CaM domains interact with synthetic peptides representing A, C and IQ of $\text{Ca}_v1.2$, leading to CDI [16]. Additional studies show that the linker region between transmembrane segments I and II of the $\text{Ca}_v1.2$ α_1 -subunit interacts with an upstream EF-hand motif on the CTT to regulate $\text{Ca}_v1.2$ in the presence of CaM [23]. Recent high resolution structures (3G43 [24], and 3OXQ [25]) show four CaM molecules bound per two peptides representing the $\text{Ca}_v1.2$ CTT. Dimerization of the CTT via coiled-coil interactions observed in the crystallographic unit cell was interpreted as an accessible physiological state by Hamilton and coworkers [24], while Minor and coworkers concluded that (a) dimerization does not occur in vitro or in vivo and (b) that the interaction of CaM with site “A” is an opportunistic, non-native interaction [25]. Thus, the number, location and thermodynamic impact of CaM-binding sites in the CTT remain controversial.

Determining the free energies of association of CaM with the CTT sites on which CaM exerts its Ca^{2+} -sensor function requires a thorough investigation of the interactions of full-length CaM (CaM_{1–148}), the CaM N-domain (CaM_{1–80}) and the CaM C-domain (CaM_{76–148}) with each of the CaM binding regions of CTT. Here we describe the binding of CaM to four synthetic peptides representing CaM-binding sites A and C and two that overlap the IQ site. To determine the effect of aromatic residues F1648 and Y1649, which precede the consensus IQ motif of $\text{Ca}_v1.2$ on interactions with CaM [14], we compared the binding affinities of CaM for two IQ peptides, one with the N-terminal anchoring residues (IQ₁₆₄₄) and one without (IQ'₁₆₅₀). To mimic fluctuation in the Ca^{2+} concentration under physiological conditions, we studied these at three levels of calcium: apo (calcium-depleted), saturating calcium (10 mM) and a low (resting) Ca^{2+} level (146 nM).

To dissect the roles of each domain of CaM, and to determine linked effects of $\text{Ca}_v1.2$ on Ca^{2+} binding to the paired sites in each domain of CaM, we conducted calcium-binding titrations of full-length (CaM_{1–148}), N-domain (CaM_{1–80}) and C-domain (CaM_{76–148}) of CaM in the presence of peptides A₁₅₈₈, C₁₆₁₄, IQ₁₆₄₄, and IQ'₁₆₅₀. This study provides a detailed thermodynamic analysis of calcium-dependent differences in the interactions of CaM with its recognition sites in $\text{Ca}_v1.2$ CTT. Integrating these findings with recent crystallographic structures and predictions of disorder tendency for the sequence of $\text{Ca}_v1.2$, we propose a new model of CaM-induced conformational change of the CTT.

2. Materials and methods

2.1. Purification of CaM

DNA encoding rat calmodulin fragments of CaM_{1–80} [26], CaM_{76–148} [27], and full-length CaM_{1–148} [28] were cloned into a pT7-7 bacterial vector and overexpressed in *Escherichia coli* Lys-S cells (U.S. Biochemicals, Cleveland, OH) as previously described [28]. All proteins were purified using Phenyl Sepharose CL-4B (Amersham Pharmacia Biotech, Piscataway, NJ) chromatography as previously described [29]. Purified proteins were dialyzed into 50 mM HEPES, 100 mM KCl and 50 μM EGTA pH 7.4. The purity of each recombinant protein was higher than 97% as assessed by reversed-phase HPLC or SDS-PAGE detected by silver staining. Protein concentrations were determined by UV absorbance in 0.1 N NaOH [30], and aliquots were stored at -20°C .

2.2. Preparation of $\text{Ca}_v1.2$ peptides

Synthetic peptides (generally referred to as $\text{Ca}_v1.2\text{p}$), with and without a 5,6-carboxyfluorescein adduct at the N-terminus of each peptide, were purchased from EZBioLab Inc. (Westfield, IN) or GenScript Corporation (Piscataway, NJ). Their compositions were as follows:

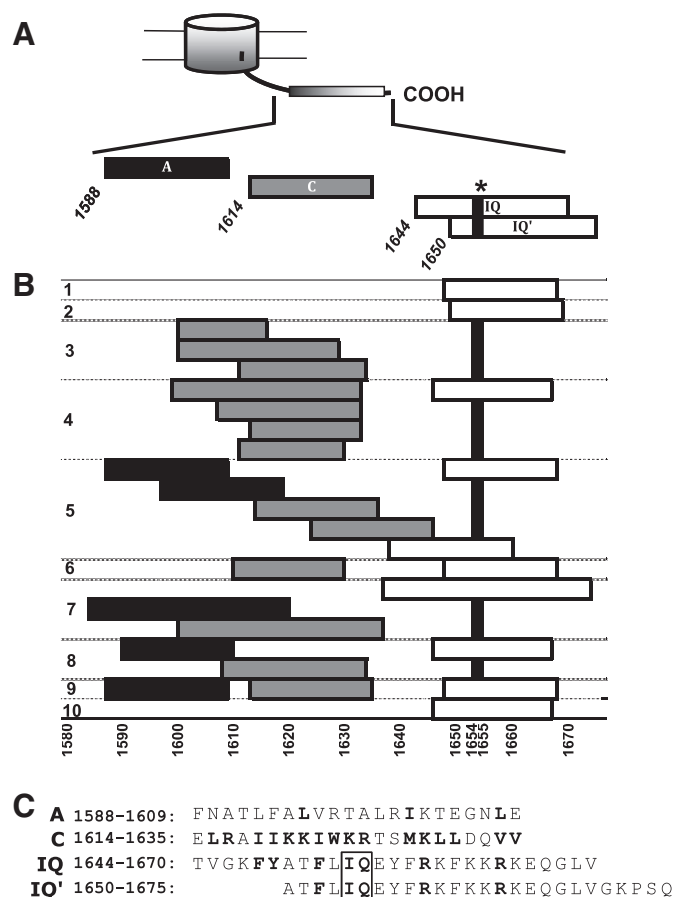


Fig. 2. Peptides from the $\text{Ca}_v1.2$ C-terminal tail (CTT) used in this study and others. (A) Schematic diagram of the CTT with the peptides used in this study represented. The asterisk (*) indicates the location of the IQ residues of the IQ motif. (B) A table of CTT peptides in the literature that are relevant to this study. (1) 1649–1668 [6], (2) 1650–1669 [19], (3) 1601–1616, 1601–1629, 1612–1634 [8], (4) Gray bars: 1600–1633, 1608–1633, 1614–1633, 1612–1630, White bar: 1647–1667 [63], (5) Black bars: 1588–1609, 1588–1619, Gray bars: 1615–1636, 1625–1646, White bars: 1649–1668, 1639–1660 [16], (6) Gray bar: 1611–1630, White bar: 1649–1668 [17], (7) Black bars: 1556–1594, 1585–1620, Gray bar: 1601–1637, White bar: 1638–1674 [21], (8) Black bar: 1591–1610, Gray bar: 1609–1634, White bar: 1647–1667 [18], (9) Black bar: 1588–1609, Gray bar: 1614–1635, White bar: 1649–1668 [23], (10) 1647–1667 [57]. (C) Sequences of the 4 peptides (A1588–1609, C1614–1635, IQ1644–1670 and IQ1650–1675) used in this study.

A₁₅₈₈ (residues 1588–1609): NH₂-Phe-Asn-Ala-Thr-Leu-Phe-Ala-Leu-Val-Arg-Thr-Ala-Leu-Arg-Ile-Lys-Thr-Glu-Gly-Asn-Leu-Glu-COOH

C₁₆₁₄ (residues 1614–1635): NH₂-Glu-Leu-Arg-Ala-Ile-Ile-Lys-Lys-Ile-Trp-Lys-Arg-Thr-Ser-Met-Lys-Leu-Leu-Asp-Gln-Val-Val-COOH

IQ₁₆₄₄ (residues 1644–1670): NH₂-Thr-Val-Gly-Lys-Phe-Tyr-Ala-Thr-Phe-Leu-Ile-Gln-Glu-Tyr-Phe-Arg-Lys-Phe-Lys-Lys-Arg-Lys-Glu-Gln-Gly-Leu-Val-Gly-Lys-Pro-Ser-Gln-COOH, and

IQ₁₆₅₀ (residues 1650–1675): NH₂-Ala-Thr-Phe-Leu-Ile-Gln-Glu-Tyr-Phe-Arg-Lys-Phe-Lys-Lys-Arg-Lys-Glu-Gln-Gly-Leu-Val-Gly-Lys-Pro-Ser-Gln-COOH.

Peptides were dissolved in distilled/autoclaved water to make stock solutions up to 1 mM. The purity of each peptide was determined by reversed-phase HPLC, and molecular weights were confirmed by MALDI-TOF. The amino acid content of each peptide was confirmed by amino acid analysis at the Molecular Analysis Facility at the Univ. of Iowa.

2.3. Analysis of binding of CaM to Ca_v1.2 peptides

Association of CaM with each of the tested Ca_v1.2 peptides was observed as an increase in the fluorescence anisotropy measured by a Fluorolog 3 (Jobin Yvon, Horiba, Inc.) spectrofluorimeter with 8 nm bandpasses and 496/520 nm excitation/emission wavelength pair (selective for fluorescein) at a temperature of 22 °C. Anisotropy (R) was calculated as indicated in Eq. (1),

$$R = \frac{I_{VV} - G \cdot I_{VH}}{I_{VV} + 2G \cdot I_{VH}} \quad (1)$$

where I_{VV} is the intensity of vertically emitted light when vertically excited, I_{VH} is the intensity of horizontally emitted light when vertically excited and G equals I_{HV}/I_{HH} where I_{HV} is the intensity of vertically emitted light when excited horizontally and I_{HH} is the intensity of horizontally emitted light when horizontally excited. The G value was calculated before each experiment and was consistently found to be 0.85 for each Fl-Ca_v1.2p. After addition of CaM, the signal was monitored for 1 s, and the average of 3 readings was calculated. Aliquots of concentrated CaM (0.5–1.2 mM) were titrated into 0.1 μM of Fl-Ca_v1.2 CTT peptides in either apo or Ca²⁺-saturated buffer. Apo buffer contained 50 mM HEPES, 100 mM KCl, 1 mM MgCl₂, 0.05 mM EGTA, 5 mM NTA (pH 7.4). Ca²⁺-saturated buffer contained all components of the apo buffer and 10 mM CaCl₂. For studies conducted at an intermediate calcium level, CaM was dialyzed multiple times against a pCa buffer that was determined experimentally to contain 146 nM free calcium. The peptide was dialyzed against the same buffer to assure that the solutions were matched. In all cases, the total dilution of the peptide solution was <3% over the course of the titrations.

To determine the affinity of CaM for Fl-Ca_v1.2p, the anisotropy data from the titration curves were fit to a simple binding model, treating the peptide–CaM complex as having a 1:1 stoichiometry. Normalized anisotropy data were plotted against the total concentration of CaM ([CaM]_{total}). The association constant was determined by fitting titration data for the effect of [CaM]_{total} on fractional change in anisotropy to a one-site Langmuir binding isotherm as described by Eq. (2),

$$\bar{Y}_1 = \frac{K_a \cdot [\text{CaM}_{\text{free}}]}{1 + K_a \cdot [\text{CaM}_{\text{free}}]} \quad (2)$$

where K_a represents the intrinsic association constant (the reciprocal of the dissociation constant, K_d) for CaM binding to a peptide, and [CaM]_{free} is the concentration of unbound CaM, calculated from the

two independent variables, [CaM]_{total} and the total concentration of Fl-Ca_v1.2p, according to the quadratic equation (Eq. (3)),

$$[\text{CaM}_{\text{free}}] = \frac{-b \pm \sqrt{b^2 - 4K_a(-[\text{CaM}_{\text{total}}])}}{2K_a} \quad (3)$$

where $b = 1 + K_a[\text{Fl-Ca}_v1.2p_{\text{total}}] - K_a[\text{CaM}_{\text{total}}]$. Under apo and intermediate calcium conditions, the affinity of CaM for Fl-Ca_v1.2p was weak, and [CaM]_{free} ≈ [CaM]_{total}. However, the affinity for Ca²⁺-saturated CaM_{1–148} was high enough that [Fl-Ca_v1.2p]_{total} ≥ 10(K_d). While this condition is appropriate for determining the stoichiometry of binding, it is not appropriate for resolving accurate affinities of binding because [CaM]_{free} is limiting. To obtain limits on the values for the affinity under those conditions, [CaM]_{free} was estimated iteratively in the nonlinear least-squares analysis [31] as the difference between [CaM]_{total} and [CaM]_{bound} (calculated as [Fl-Ca_v1.2p]_{total} • \bar{Y}_1). To account for the effect of change in volume over the titration, the value of [Fl-Ca_v1.2p]_{total} was corrected for dilution and included as a second independent variable in the nonlinear least-squares analysis. Eq. (4) accounted for experimental variations in the observed end points of individual titration curves:

$$\text{Signal} = f(X) = Y_{[X]_{\text{low}}} + \bar{Y}_1 \cdot [(Y_{[X]_{\text{high}}} - Y_{[X]_{\text{low}}}) = \text{Span}] \quad (4)$$

where \bar{Y}_1 refers to average fractional saturation of the peptide and $Y_{[X]_{\text{low}}}$ corresponds to the intrinsic fluorescence anisotropy of Fl-Ca_v1.2p in the absence of CaM. The *Span* describes the magnitude and direction of signal change upon titration (i.e., the difference between the high ($Y_{[X]_{\text{high}}}$) and low ($Y_{[X]_{\text{low}}}$) endpoints). The *Span* was positive for increasing anisotropy. The endpoint or upper limit of data was fit directly in the analysis of titrations that were conducted with Ca²⁺-saturated CaM.

Titration of A₁₅₈₈, C₁₆₁₄, IQ₁₆₄₄, and IQ₁₆₅₀ with apo CaM did not give a well-defined upper plateau for fitting the experimental data to Eq. (3). Therefore, the final apo CaM:peptide complex was titrated with CaCl₂ (in matching buffer) to a final concentration of 10 mM. The value of raw anisotropy obtained from the resulting calcium-saturated CaM:Ca_v1.2p complex was then treated as the upper endpoint (i.e., set to 1) in the nonlinear least-squares analysis of those titrations. Ultimately, for titrations showing a very small change in anisotropy (i.e., minimal binding of apo CaM), it was only possible to put a limit on the possible dissociation constant. In Figs. 3 and 4, a diamond at the upper asymptote is included to signify this approximation.

2.4. Hydrodynamic T₂ relaxation experiment as detected by ¹⁵N HSQC

A uniformly labeled sample of ¹³C, ¹⁵N CaM_{1–148} (1 mM) saturated with IQ₁₆₄₄ in 10 mM deuterated imidazole, 100 mM KCl, 0.01% azide, 10 mM CaCl₂, 10% D₂O pH 6.5 was used. Amide chemical shifts for CaM_{1–148} saturated with Ca_v1.2p were confirmed by the following 2D and 3D experiments: ¹⁵N-HSQC, HNCACB, HNCOCACB, HNCACO, HNCO, HNCA, HNCOCACB, CCONH (TOCSY). 3D NMR data were collected on an 800 MHz Bruker spectrometer at the NMR facility in the University of Iowa, College of Medicine. T₂ relaxation experiments were collected on a 600 MHz Varian spectrometer. A total of 9 ¹⁵N HSQC experiments were performed for T₂ analysis. T₂ values (in ms) were extracted by measuring the intensities of cross-peaks in 2D maps as a function of a relaxation delay and fitted to a two-parameter monoexponential function with the NMRViewJ software for data analysis and visualization [32]. The pulse delays (T) were 0, 17.28, 34.56, 51.84, 69.12, 86.40, 103.68, 138.24 and 172.80 ms.

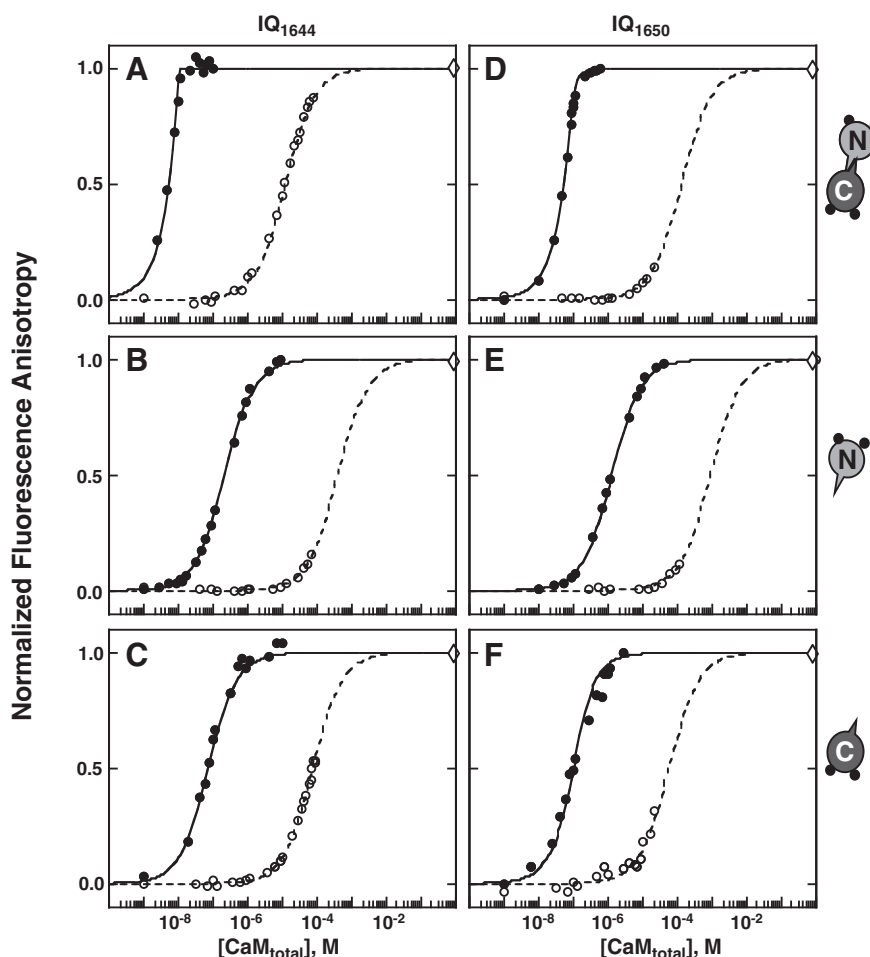


Fig. 3. Titrations of FI-IQ₁₆₄₄ and FI-IQ₁₆₅₀ with CaM. Titrations with (A and D) CaM_{1–148}, (B and E) CaM_{1–80} and (C and F) CaM_{76–148} monitored by fluorescence anisotropy. Titrations of FI-IQ₁₆₄₄ with CaM under calcium-saturated conditions (10 mM CaCl₂) were carried out with 0.01 μM peptide. Titrations of FI-IQ₁₆₅₀ were performed with 0.1 μM FI-Ca_v1.2p. Titrations were performed in 50 mM HEPES, 100 mM KCl, 1 mM MgCl₂, 0.05 mM EGTA, 5 mM NTA, pH 7.4 at 22 °C. Data for apo CaM (○, dashed line) is compared to calcium-saturated CaM (10 mM CaCl₂; ●, solid line). Diamond on the right axis indicates that asymptote was estimated by addition of excess calcium, CaM or both.

2.5. Fluorescence-monitored equilibrium Ca²⁺ titrations

Equilibrium Ca²⁺-titrations were conducted with a PTI fluorimeter (Photon Technology International, Lawrenceville, NJ) with a xenon lamp, using 8 nm band passes to measure changes in the Ca²⁺ affinity of CaM in the presence and absence of each tested Ca_v1.2p. Samples contained either 2 μM CaM alone (CaM_{1–148}, CaM_{1–80} and CaM_{76–148}) or with 6 to 8 μM Ca_v1.2p (1:3 or 1:4 CaM:Ca_v1.2p molar ratio) in 50 mM HEPES, 100 mM KCl, 1 mM MgCl₂, 0.05 mM EGTA, 5 mM NTA, pH 7.4 at 22 °C. Using a microburet (Micro-Metric Instrument Co., Cleveland, OH) fitted with a 250 μl Hamilton syringe (Hamilton Co., Reno, NV), CaM:peptide samples were titrated with concentrated calcium solutions (~5 mM, 50 mM or 500 mM CaCl₂ in the same buffer that was used throughout the titrations). Calcium binding to the N-domain (sites I and II) was monitored by a decrease in intrinsic Phe fluorescence (λ_{ex} of 250 nm, λ_{em} of 280 nm). For calcium titrations conducted in the presence of 3 peptides (A₁₅₈₈, IQ₁₆₄₄, and IQ₁₆₅₀), calcium binding to the C-domain (sites III and IV) was monitored by intrinsic Tyr fluorescence using wavelengths (λ_{ex} of 277 nm, λ_{em} of 320 nm) as previously described [33]. Under these conditions, there is no calcium-dependent change in fluorescence intensity of phenylalanine residues in the C-domain. For calcium titrations of CaM in the presence of C₁₆₁₄, we monitored Tyr fluorescence at different wavelengths (λ_{ex} of 270 nm, λ_{em} of 285 nm) to reduce possible interference caused by the presence of a tryptophan residue in the peptide.

For each calcium addition, the free calcium concentration was determined using Eq. (5). This expression relates the fractional saturation of a fluorescent calcium-indicator dye in the sample to the concentration of free calcium.

$$[Ca^{2+}]_{free} = K_d \frac{[Indicator : Ca^{2+}]}{[Indicator]_{free}} \quad (5)$$

In this study, 0.1 μM Oregon Green (Molecular Probes, Eugene, OR) was used for calcium titrations of CaM alone (no peptide), and 0.05 μM XRhod5F (Molecular Probes, Eugene, OR) was used for titrations in the presence of Ca_v1.2p. The K_d values of calcium dissociation from Oregon Green (34.24 μM) and XRhod5F (1.78 μM) were determined experimentally in 50 mM HEPES, 100 mM KCl, 1 mM MgCl₂, pH 7.4 at 22 °C. Atomic absorption spectroscopy was used to determine contaminating calcium in the buffer, as well as the exact calcium concentrations of titrant solutions. Each calcium titration was repeated three to eight times; averages and standard deviations were reported in Table 2. XRhod5F was used as an indicator in calcium titrations of CaM in the presence of Ca_v1.2p because of its ~20-fold lower K_d (higher affinity for calcium).

2.6. Analysis of the free energy (ΔG₂) of calcium binding to CaM

The fluorescence intensity readings for each titration were subjected to nonlinear least-squares analysis using NONLIN [31] to

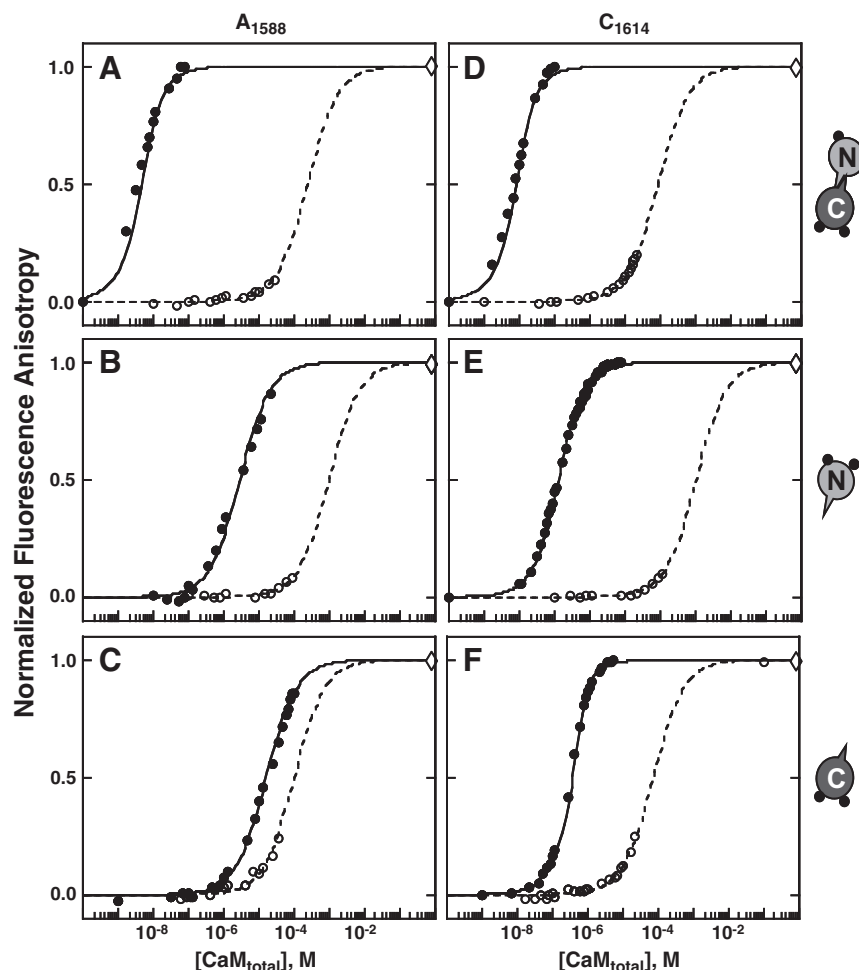


Fig. 4. Titrations of FI-A₁₅₈₈ and FI-C₁₆₁₄ with CaM. Titrations of 0.1 μ M FI-Ca_v1.2p with (A and D) CaM_{1–148}, (B and E) CaM_{1–80} and (C and F) CaM_{76–148} monitored by fluorescence anisotropy. Titrations were performed in 50 mM HEPES, 100 mM KCl, 1 mM MgCl₂, 0.05 mM EGTA, 5 mM NTA, pH 7.4 at 22 °C. Data for apo CaM (○, dashed line) is compared to calcium-saturated CaM (10 mM CaCl₂; ●, solid line). Diamond on the right axis indicates that asymptote was estimated by addition of excess calcium, CaM or both.

determine the free energies of calcium binding (ΔG_1 and ΔG_2) to the N-domain (sites I and II) and the C-domain (sites III and IV). Data were fit to a two-site Adair function as given in Eq. (6),

$$\bar{Y}_2 = \frac{K_1 \cdot [X] + 2 \cdot K_2 [X]^2}{2(1 + K_1 \cdot [X] + K_2 \cdot [X]^2)} \quad (6)$$

where the pair of sites within a domain (i.e., sites I and II in the N-domain or sites III and IV in the C-domain) are allowed to be non-identical and cooperative [28]. The macroscopic equilibrium constant K_1 ($\Delta G_1 = -RT \ln K_1$) in Eq. (5) represents the sum of two intrinsic constants (k_1 and k_2) that may or may not be equal. The macroscopic constant K_2 ($\Delta G_2 = -RT \ln K_2$) represents the equilibrium constant for calcium binding to both sites (the product of k_1 , k_2 and k_{12}) and accounts for any positive or negative cooperativity.

In the absence of Ca_v1.2p, the overall change in the Phe signal (λ_{ex} of 250 nm, λ_{em} of 280 nm) represents calcium binding solely to the N-domain (sites I and II) [34]. Therefore, the equilibrium calcium-titration data were fit to a function $[f(X)]$ describing fluorescence intensity signal as shown in Eq. (7).

$$f(X) = Y_{[X]_{\text{low}}} + \bar{Y}_2 \cdot \text{Span} \quad (7)$$

where $Y_{[X]_{\text{low}}}$ corresponds to the value of fluorescence intensity at the lowest calcium concentration and *Span* accounts for the magnitude

and direction of signal change upon increasing calcium concentration (e.g., usually increasing magnitude of intensity for Tyr signal, and decreasing magnitude for Phe signal).

In the presence of peptides A₁₅₈₈, C₁₆₁₄, and IQ'1650, Tyr no longer fully quenched the steady-state fluorescence intensity of the Phe residues in the C-domain of CaM, and the intensity of the Phe signal from CaM_{76–148} decreased in a calcium-dependent manner in parallel with the increasing Tyr signal. Thus, we treated the total Phe intensity (A_T) of CaM_{1–148} in the presence of each Ca_v1.2p as the sum of an intensity change (A_C) attributed to the C-domain, and another (A_N) representing the signal change of the N-domain upon calcium binding.

$$A_T = A_N + A_C \quad (8a)$$

The free energy of calcium binding to the N-domain of CaM_{1–148} was determined using Eq. (8b),

$$f(X) = Y_{[X]_{\text{low}}} + \text{Span} \cdot ([A_N / A_T] \cdot \bar{Y}_N + [A_C / A_T] \cdot \bar{Y}_C) \quad (8b)$$

which takes into account the sum of two Adair equations (\bar{Y}_N and \bar{Y}_C) multiplied by the corresponding fractional contributions of each domain to the total amplitude of the intensity change (i.e., $[A_N / A_T] \cdot \bar{Y}_N$ and $[A_C / A_T] \cdot \bar{Y}_C$). The fractional contribution of the N-domain to the

total intensity change is simply $(1 - A_C/A_T)$. Therefore, Eq. (8b) can be rewritten as follows:

$$f(X) = Y_{[X]_{low}} + Span \cdot [(1 - [A_C/A_T]) \cdot \bar{Y}_N + [A_C/A_T] \cdot \bar{Y}_C]. \quad (8c)$$

The fluorescence intensity contribution of calcium binding to sites III and IV within the C-domain of CaM_{1–148} was calculated by comparing the Phe signal intensity determined from equilibrium calcium-titrations of full-length CaM_{1–148} (A_T) and the isolated domain CaM_{76–148} (A_C), using the same buffer conditions and instrument settings. The value of A_C was treated as being the same as the amplitude of the intensity change for CaM_{76–148}. The fractional contribution of the C-domain Phe signal to the total amplitude intensity (A_C/A_T) was determined to be 32% for A₁₅₈₈, 7.8% for C₁₆₁₄, and 18% for IQ₁₆₅₀.

3. Results and discussion

The previously determined CaM-binding sites of the Ca_v1.2 α_1 -subunit CTT are localized to three regions spanning approximately 90 amino acids (Fig. 2A). Laboratories studying Ca_v1.2 have reported distinct but overlapping sequences of the CTT as sites for CaM interactions. These results are summarized in Fig. 2B. The amino acid sequences of the four peptides used in this study are shown in Fig. 2C, where basic, hydrophobic and IQ-motif residues are shown in bold.

While association of CaM with the IQ-motif of Ca_v1.2 CTT has been shown to occur during resting conditions in the cell, as well as during a spike of calcium [18,21,22], the interactions of CaM with the “A” and “C” sites (corresponding to A₁₅₈₈ and C₁₆₁₄) remain unclear despite increasing structural detail ([24], [25]). To better understand the calcium-dependent role of these sites in recruiting or repositioning CaM on the α_1 -subunit of Ca_v1.2 CTT, we compared the association characteristics of full-length CaM_{1–148}, N-domain CaM_{1–80} and C-domain CaM_{76–148} with synthetic peptides representing the CaM-binding sites on the CTT of Ca_v1.2 under Ca²⁺-saturating and apo conditions. However, to mimic resting conditions, which have a low (submicromolar) level of calcium, we also monitored interactions of CaM_{1–148} with Ca_v1.2 CTT peptides at an intermediate level of Ca²⁺ (146 nM). A unique feature of this study is that we report the linked effect of these channel-CaM associations on the Ca²⁺ affinity of each pair of sites within wild-type CaM_{1–148} and compare those to effects on the individual domains of CaM.

3.1. CaM binding to FI-IQ₁₆₄₄ and FI-IQ₁₆₅₀

IQ motif peptides of the Ca_v1.2 CTT are known to bind CaM with high affinity. We investigated the energetic contributions of upstream hydrophobic residues of the IQ motif by studying CaM binding to two overlapping peptides. IQ₁₆₅₀ excluded these residues, while IQ₁₆₄₄ contained them (see Figs. 1 and 2).

CaM can interact with IQ-motifs under apo conditions [35]. CaM targets containing IQ motifs include ion channels [21], myosin [36], and neuromodulin [37]. The CaM binding site of these proteins contains the consensus IQ motif (IQXXRGXXR), where X represents any amino acid. For some voltage-gated ion channels, this region is sufficient to mediate high affinity binding of CaM via its C-domain, as seen in recent solution structures that show the C-domain of apo CaM adopting a semi-open conformation when bound to IQ motifs from the Na_v1.2 [38] and Na_v1.5 [39] voltage-gated sodium channels.

Although residues within the Ca_v1.2 IQ motif were shown to alter CaM binding and activity of Ca_v1.2 [40], increasing evidence shows that residues near, but outside, of the consensus IQ motif also contribute to the energy and specificity of CaM binding [41,42]. A CSU analysis of the CaM-peptide contacts in the crystal structure (2IX7) of two apo CaM molecules bound to the first two IQ motifs of murine myosin V showed that non-consensus IQ-motif residues interact with

both domains of CaM [36] as diagrammed in Fig. 1E and F. These residues also affected the Ca²⁺-dependent dissociation properties of CaM from the IQ motifs of myosin V [43,44]. Fig. 1D shows a CSU analysis of a crystal structure (2BE6) of Ca²⁺-saturated CaM bound to the IQ motif of the Ca_v1.2 CTT [13,14]. There are many contacts between CaM and the sequence preceding the IQ motif. Three of these are between aromatic residues (Phe1648, Tyr1649 and Phe1652) in the peptide that make extensive hydrophobic contacts with residues in the N-domain of CaM (indicated in blue). Structures of Ca²⁺-saturated CaM in complex with peptides containing IQ motifs from P/Q-(Ca_v2.1), N-(Ca_v2.2) and R-(Ca_v2.3) type Ca²⁺-channels also identified non-consensus residues upstream of the IQ motif that were necessary for proper channel function [41,42], although these studies disagree regarding the orientation of the lobes of CaM upon binding.

To determine the effect of non-consensus residues located upstream of the Ca_v1.2 CTT IQ-motif on the interactions with CaM_{1–148}, CaM_{1–80} and CaM_{76–148}, we measured the binding affinity of CaM for the two peptides: FI-IQ₁₆₄₄, which contains all of the anchoring residues (Phe1648, Tyr1649 and Phe1652) previously shown to interact with the N- and C-domains of CaM [14,42] and FI-IQ₁₆₅₀, which contains only one of the anchoring residue (Phe1652) at the N-terminal region of the peptide and an additional five amino acids at the C-terminal region.

Under Ca²⁺-saturating conditions, the binding affinity of FI-IQ₁₆₄₄ for CaM_{1–148} was the most favorable observed for all peptides studied (Fig. 3A). The titration was completely stoichiometric. The K_d estimated for a one-site binding isotherm was lower than 1 nM. (As will be explained below, after conducting calcium titrations of the CaM:IQ complex, we revised this estimate to be to ≤ 1 pM.) Under these conditions, CaM_{1–148} bound to FI-IQ₁₆₄₄ with a 1:1 stoichiometry. The binding affinities of FI-IQ₁₆₄₄ for CaM_{1–80} (Fig. 3B) and CaM_{76–148} (Fig. 3C) were also favorable (K_d of 0.21 ± 0.003 μ M and 0.08 ± 0.006 μ M, respectively) under Ca²⁺-saturating conditions.

In this study, the most favorable binding affinity of apo CaM was observed for FI-IQ₁₆₄₄ binding to CaM_{1–148} (K_d of 13.5 ± 2.1 μ M). FI-IQ₁₆₄₄ had a weaker binding affinity for CaM_{1–80} and CaM_{76–148} under apo conditions, with calculated K_d values ranging from 55 to 375 μ M (Table 1).

Table 1
Equilibrium constants^a for CaM dissociation from FI-Ca_v1.2p.

Peptide	Calcium-saturated ^b	“Resting” Ca ²⁺ ^c	Apo ^d
FI-A ₁₅₈₈			
CaM _{1–148}	≤ 2 nM	516 ± 236	215 ± 38
N (CaM _{1–80})	2.41 ± 0.32	– ^e	1580 ± 439
C (CaM _{76–148})	14.4 ± 6.42	– ^e	98 ± 16
FI-C ₁₆₁₄			
CaM _{1–148}	≤ 2 nM	4.1 ± 0.37	85 ± 35
N (CaM _{1–80})	≤ 70 nM	– ^e	1230 ± 181
C (CaM _{76–148})	≤ 70 nM	– ^e	65 ± 4.3
FI-IQ ₁₆₄₄			
CaM _{1–148}	≤ 1 pM ^f	1.4 ± 0.14	13.5 ± 2.1
N (CaM _{1–80})	0.21 ± 0.003	– ^e	375 ± 20
C (CaM _{76–148})	0.08 ± 0.006	– ^e	55 ± 18
FI-IQ ₁₆₅₀			
CaM _{1–148}	≤ 2 nM	2.5 ± 0.18	119 ± 32
N (CaM _{1–80})	1.1 ± 0.97	– ^e	804 ± 103
C (CaM _{76–148})	≤ 10 nM	– ^e	55 ± 15

^a K_{dssn} values have units of μ M unless specified otherwise. Standard buffer was augmented with ^b10 mM CaCl₂, ^c146 nM CaCl₂ (concentration determined experimentally using indicator dyesdip-BAPTA and Oregon Green), or ^dcalcium-depleted by dialysis against 5 mM EGTA/NTA. ^eNot determined. ^fBinding was stoichiometric and the experimentally estimated K_d was lower than 1 nM. The reported limit of 1 pM was inferred from linkage calculations for calcium binding to CaM alone, and the CaM:IQ complex, and peptide binding to apoCaM.

We note that the binding affinity of Ca^{2+} -saturated CaM_{1-148} for FI-IQ_{1650} (which contains one of the hydrophobic anchoring residues [Phe1652]) was nearly two orders of magnitude weaker than that of FI-IQ_{1644} (Fig. 3D). However, the binding was still very favorable, with an estimated K_d of ≤ 2 nM. The binding affinity of CaM_{76-148} for IQ_{1650} (Fig. 3E) was about 100-fold more favorable than that of CaM_{1-80} (Fig. 3F) under Ca^{2+} -saturating conditions ($K_d \leq 10$ nM and 1.10 ± 0.97 μM , respectively).

The dissociation constant for apo CaM_{1-148} binding to FI-IQ_{1650} (K_d of 119 ± 32 μM) was about 9-fold less favorable than that for binding to FI-IQ_{1644} (K_d of 13.5 ± 2.1 μM ; Fig. 3D). The dissociation constants for apo CaM_{76-148} binding to FI-IQ_{1650} and FI-IQ_{1644} were identical (K_d of 55 ± 15 μM and 55 ± 18 μM , respectively). Similar to the comparison of Ca^{2+} -saturated domains, apo CaM_{1-80} had a less favorable affinity for FI-IQ_{1650} (K_d of 804 ± 103 μM) than for FI-IQ_{1644} (K_d of 375 ± 20 μM) (Fig. 3E).

From these results, it is clear that residues outside of the consensus IQ-motif mediate important contacts with the domains of CaM. The binding affinity of CaM_{1-80} for FI-IQ_{1644} is more favorable than for FI-IQ_{1650} under both apo and Ca^{2+} -saturated conditions, suggesting that residues outside of the consensus IQ-motif located in the N-terminal region interact with the N-domain of CaM_{1-148} to form an energetically tight complex. These results are in agreement with a model that indicates CaM binding parallel to the IQ motif on the CTT of $\text{Ca}_v1.2$, where the interactions of the N-domain of CaM are mediated by the N-terminal part of the IQ-motif.

3.2. CaM binding to pre-IQ sites – A_{1588} and C_{1614}

The “A” and “C” sites located in the $\text{Ca}_v1.2$ CTT α_1 -subunit were previously shown to associate with the N-domain of CaM_{1-148} when [calcium] was 20–100 nM [16], and with the C-domain of Ca^{2+} -saturated CaM [18]. Pitt and co-workers suggested that the EF-hand motif of the CTT mediates the binding of apo and Ca^{2+} -saturated CaM to upstream recognition sites [23], while more recently Minor and coworkers have suggested that site A may be a non-native, fortuitous site [25]. To better understand the domain-specific interactions of CaM with these two “pre-IQ” regions, we determined the affinity of FI-A_{1588} and FI-C_{1614} for full-length CaM_{1-148} , N-domain CaM_{1-80} and C-domain CaM_{76-148} , under Ca^{2+} -saturating and apo conditions (Fig. 4 and Table 1).

FI-A_{1588} (Fig. 4A) had a very favorable affinity for Ca^{2+} -saturated CaM_{1-148} . Limitations related to observable signal from fluorescein required a concentration of peptide that was determined to be higher than the apparent K_d ; thus, the binding was stoichiometric. Replicate titrations were compared to a one-site binding isotherm with an estimated dissociation constant (K_d) of ≤ 2 nM based on analysis that accounted for peptide concentration. This is necessarily only a limit. The actual dissociation constant may be lower (more favorable).

To determine the specificity of FI-A_{1588} for domains of CaM, we measured its affinity for Ca^{2+} -saturated N-domain CaM_{1-80} (Fig. 4B) and C-domain CaM_{76-148} (Fig. 4C). FI-A_{1588} had a much weaker affinity for each individual EF-hand domain of CaM (K_d of 2.41 ± 0.32 μM for CaM_{1-80} and K_d of 14.4 ± 6.4 μM for CaM_{76-148}) as compared to full-length CaM_{1-148} . Although the N-domain of CaM has been reported to be sufficient to promote initial attachment and activation of CaMKII [45], in most cases where there is a difference between the domains of CaM, it is the interaction of a target with the C-domain of CaM that is more energetically favorable. Thus, the observation that the N-domain of CaM binds to FI-A_{1588} with a 6-fold more favorable equilibrium constant than that of the CaM C-domain is unusual compared to the majority of CaM target interactions. Given that the affinity of full-length CaM is more favorable than 2 nM, we expect that this difference will orient the N-domain to bind at site “A”.

To test the affinity of apo CaM for FI-A_{1588} , we performed similar experiments in a buffer depleted of Ca^{2+} using apo CaM titrant that had been extensively dialyzed against calcium chelators. In contrast to

the results obtained for Ca^{2+} -saturated CaM, apo FI-A_{1588} had a very weak affinity for all CaM fragments tested (Fig. 4, dashed curves, Table 1), with the weakest obtained with CaM_{1-80} . In these titrations, we note that the maximal concentration of CaM exceeded 100 μM in most cases, but the final measured anisotropy value (R) was less than 20% of the overall anisotropy change determined by comparing results to the titrations with Ca^{2+} -saturated CaM (see *Materials and methods* for description). Estimates of the most favorable K_d values consistent with titrations of apo CaM binding were in the range of high μM to low mM, indicating that association of apo CaM exclusively with the “A” site would be unlikely under physiological conditions.

Similar to the affinity determined for FI-A_{1588} binding to Ca^{2+} -saturated CaM_{1-148} , that of FI-C_{1614} for Ca^{2+} -saturated CaM_{1-148} was very favorable ($K_d \leq 3$ nM), and the titration was stoichiometric (Fig. 4D). However, in contrast to the binding of FI-A_{1588} to individual domains of CaM, FI-C_{1614} had a more favorable affinity for both Ca^{2+} -saturated CaM_{1-80} (Fig. 4E) and Ca^{2+} -saturated CaM_{76-148} (Fig. 4F), with the estimated $K_d \leq 70$ nM for each domain. Apo CaM_{1-148} had a weak affinity for FI-C_{1614} (Fig. 4D – dashed line). The affinities of apo CaM_{1-80} and apo CaM_{76-148} for FI-C_{1614} were comparable to their affinities for FI-A_{1588} , and were considered insufficient to mediate association independently under physiological conditions (Table 1). However, avidity might allow interactions in this region if one domain were anchored at A and the other at C.

The affinity of FI-A_{1588} for apo CaM is much less favorable than that previously reported by Pitt and coworkers who analyzed peptide binding to dansylated CaM [16,23]. However, our studies agree in finding that peptide “A” bound more favorably to an N-domain

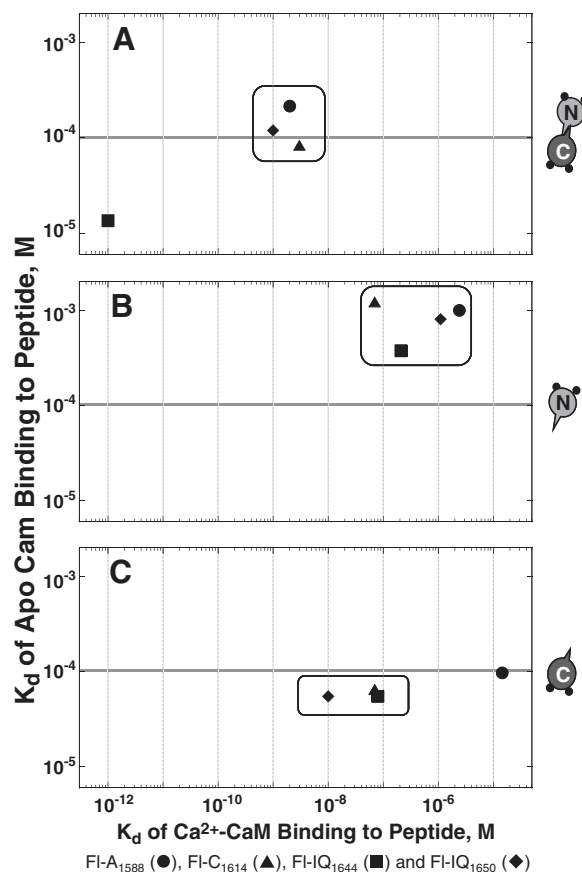


Fig. 5. CaM binding to $\text{FI-Ca}_v1.2p$. Comparison of dissociation constants (K_d) for the binding of (A) CaM_{1-148} , (B) CaM_{1-80} and (C) CaM_{76-148} to FI-A_{1588} (●), FI-C_{1614} (▲), FI-IQ_{1644} (■) and FI-IQ_{1650} (◆) under calcium-saturated (X-axis) and apo (Y-axis) conditions.

fragment of CaM than a C-domain fragment [16]. The stoichiometric binding of Fl-A₁₅₈₈ and Fl-C₁₆₁₄ to CaM_{1–148} under Ca²⁺-saturating conditions suggests that these two pre-IQ sites bind CaM when Ca²⁺ levels are elevated such that at least one domain is calcium-saturated.

A summary plot representing dissociation constants (K_d) of CaM_{1–148}, CaM_{1–80} and CaM_{76–148} for all four peptides tested for both apo (Y-axis) and Ca²⁺-saturating (X-axis) conditions is shown in Fig. 5. The energies of binding IQ₁₆₄₄ to both apo and Ca²⁺-saturated CaM_{1–148} were the most favorable of all associations determined in this study (Fig. 5A). The dissociation constant for calcium-saturated CaM could not be measured directly, and was clearly more favorable than 1 nM. The estimate (1 pM) reported in Table 1 was based on linkage analysis of calcium binding to the CaM:IQ complex, which is described below. These findings are similar to our observations of Ca²⁺-saturated CaM binding to its preferred site in β -calcineurin; the isolated N- and C-domains each had a K_d of ~ 1 μ M, while the K_d of full-length CaM was ~ 1 pM (i.e., the square of 1 μ M) [46]. Under apo conditions, all of the peptides bound more weakly to apo CaM_{1–80}, than to CaM_{1–148} and CaM_{76–148}. Notably, under calcium-saturating conditions, A₁₅₈₈ had a higher affinity for CaM_{1–80} than for CaM_{76–148} (Fig. 5B and C), suggesting that positioning of the N-domain within (Ca²⁺)₄-CaM_{1–148} contributes more of the specificity in recognition of A₁₅₈₈.

3.3. CaM_{1–148} binding Ca_v1.2p at low [Ca²⁺] in resting cells

Previous studies of the association properties of CaM and Ca_v1.2 CTT peptides have suggested that at least 10 to 100 nM Ca²⁺ is required for significant binding [16]. Resting rat ventricular free Ca²⁺ concentrations in vivo have been reported between 121 nM [47] and 181 nM [48]. To simulate these in vivo resting Ca²⁺ concentrations, we measured the binding affinity of CaM_{1–148} for Fl-A₁₅₈₈, Fl-C₁₆₁₄, Fl-IQ₁₆₄₄ and Fl-IQ₁₆₅₀ in the presence of 146 nM of Ca²⁺. Fl-A₁₅₈₈ had the weakest affinity for CaM_{1–148} with a K_d of 516 μ M (Fig. 6A). The affinities of Fl-C₁₆₁₄ (K_d = 4.06 μ M) (Fig. 6B), Fl-IQ₁₆₄₄ (K_d = 1.40 μ M)

(Fig. 6C), and Fl-IQ₁₆₅₀ (K_d = 2.53 μ M) (Fig. 6D) were more favorable for CaM_{1–148}. Overall, the weak affinity of Fl-A₁₅₈₈ for CaM_{1–148} suggests that this site is not utilized in isolation by CaM at resting intracellular Ca²⁺ levels. Values for the dissociation constants determined for Fl-C₁₆₁₄, Fl-IQ₁₆₄₄ and Fl-IQ₁₆₅₀ for CaM_{1–148} under low Ca²⁺ conditions agree with previous reports, which suggest that these motifs serve as so called “pre-association” sites for CaM on Ca_v1.2 CTT. For the IQ motif, it has been reported that CaM with one lobe Ca²⁺ saturated, as it would be at resting calcium concentrations, binds to and mediates the response of Ca_v1.2 to Ca²⁺ [49].

3.4. Stoichiometry of Ca²⁺-saturated CaM_{1–148}–IQ₁₆₄₄ complex

CaM binding to the CTT of Ca_v1.2 regulates channel opening, and one CaM molecule was shown to be sufficient for mediating the activity [50]. Recent structural studies demonstrate that it is possible to load the CTT with at least two molecules of CaM [24] [51]. To investigate the presence of non-specific interactions between CaM and Ca_v CTT peptides, we studied the stoichiometry of the highest affinity Ca²⁺-saturated CaM_{1–148}:IQ₁₆₄₄ complex. For all titrations of Fl-IQ₁₆₄₄ with CaM_{1–148} monitored by fluorescence anisotropy, the ratio of [CaM]:[IQ₁₆₄₄] was 1:1 but this ratio is identical to that of a 2:2 complex.

To test whether a 1:1 complex forms between CaM_{1–148} and IQ₁₆₄₄ at higher concentrations of IQ₁₆₄₄ and CaM, we performed 2D-HSQC NMR experiments to determine the transverse relaxation parameter (T_2) of the Ca²⁺-CaM_{1–148}–IQ₁₆₄₄ ternary complex and compared it with T_2 value of CaM: CaM/dependent kinase II peptide (CaMKIIp), which is a known 1:1 complex.

Experiments were performed as described in the *Materials and methods* section. Backbone assignments of a uniformly labeled ¹³C¹⁵N-rCaM_{1–148} sample saturated with IQ₁₆₄₄ and Ca²⁺ were made using standard triple-resonance experiments (described in *Materials and methods* section). Ca²⁺-saturated ¹³C¹⁵N-rCaM_{1–148} was titrated with

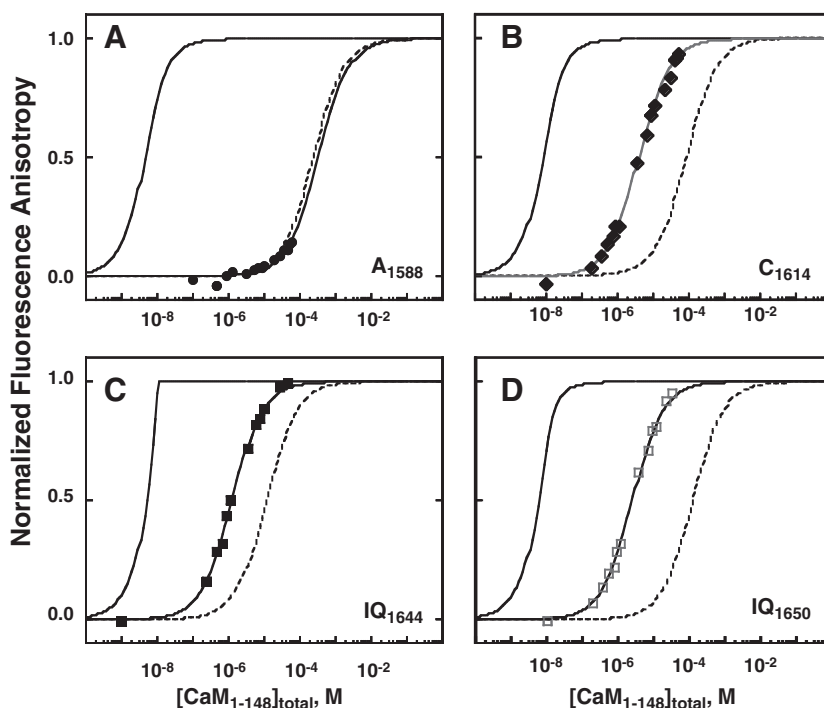
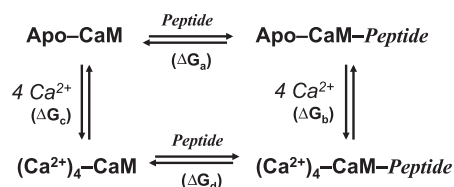


Fig. 6. Titrations of Fl-Ca_v1.2p with CaM_{1–148} under low (resting) [Ca²⁺] (146 nM). Normalized anisotropy of (A) Fl-A₁₅₈₈ (●), (B) C₁₆₁₄ (▲), (C) IQ₁₆₄₄ (■) and (D) IQ₁₆₅₀ (◆) upon titrating with CaM_{1–148} at a low calcium-concentration. Titrations of (A) and (B) were carried out with 0.1 μ M peptide. Titrations of (C) and (D) were carried out with 0.01 μ M peptide. All peptides were tested in 50 mM HEPES, 100 mM KCl, 1 mM MgCl₂, 0.05 mM EGTA, 5 mM NTA, pH 7.4 at 22 °C, with 146 nM calcium. Titrations under apo (dashed lines) and calcium-saturated (solid lines) conditions are shown as a reference.

IQ₁₆₄₄ to the point of saturation and monitored using ¹⁵N HSQC NMR. The peaks of CaM followed a slow-exchange regime (i.e., tight binding of CaM to the peptide) throughout the titration with IQ₁₆₄₄, which confirmed the estimate of an extremely favorable dissociation constant ($K_d \leq 1$ pM) for CaM_{1–148} and IQ₁₆₄₄ previously estimated by anisotropy studies (Fig. 4A). The concentration of CaM used in this experiment was approximately 1 mM, 5 orders of magnitude higher than the concentration (10 nM) of IQ₁₆₄₄ used in the fluorescence anisotropy experiments. SI Fig. 1A represents the measured ¹⁵N relaxation parameter as a function of CaM residues in complex with IQ₁₆₄₄, and the histogram (frequency versus bin) is shown in SI Fig. 1B. For most residues, T_2 values range from 60 to 80 ms. Residues from both N- and C-domains of CaM experience similar motion when in complex with IQ₁₆₄₄ (SI Fig. 1B). The average T_2 value was 68 ms. This value is comparable to the results obtained when the CaM–CaMKIIp complex was monitored under Ca²⁺-saturating conditions, in which T_2 was determined to be 77 ms and the association of CaM with melittin and its binding domain from calcineurin [46]. In conclusion, these results indicate that Ca²⁺-saturated CaM forms a uniform 1:1 complex with CavIQ₁₆₄₄, as determined from both fluorescence anisotropy and the T_2 analysis of the backbone dynamics. The stoichiometry of CaM–IQ₁₆₄₄ is not dependent on the concentration of CaM or peptide used in the experiment. This analysis is, however, consistent with proposals that two CaM molecules may bind to Cav1.2 simultaneously by interacting at the pre-IQ region (sites “A” and “C”).

3.5. Effect of Cav1.2p on the Ca²⁺-binding sites of CaM

Association of CaM with target proteins differentially affects the Ca²⁺-affinity of the domains of CaM. Some targets enhance the Ca²⁺-binding affinity [52–54], whereas others decrease the affinity [55,56]. This is summarized by the linkage scheme below.



The domain-dependent modulation of Cav1.2 by CaM is highly sensitive to the Ca²⁺-binding affinity of the domains [11]. CaM responds to binding sites in Cav1.2 by adjusting its Ca²⁺-binding affinity and plays an important role in mediating the Ca²⁺-dependent inactivation (CDI) and Ca²⁺-dependent facilitation (CDF). We performed fluorescence-monitored equilibrium Ca²⁺ titrations of CaM in the presence and absence of Cav1.2 CTT peptides to determine how the Ca²⁺-binding affinity of CaM_{1–148}, CaM_{1–80} and CaM_{76–148} were altered upon peptide binding.

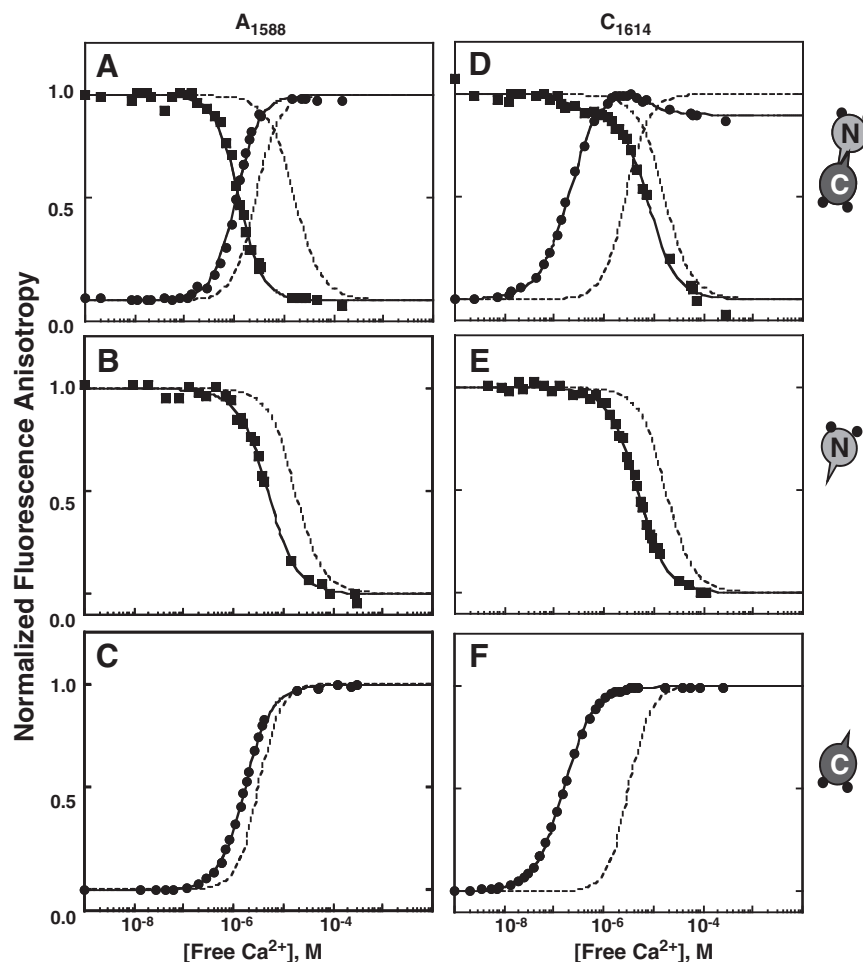


Fig. 7. Equilibrium Ca²⁺-titrations of CaM and A₁₅₈₈ or C₁₆₁₄. Titrations of (A and D) CaM_{1–148}, (B and E) CaM_{1–80} and (C and F) CaM_{76–148} in the presence of (A, B, C) A₁₅₈₈ and (D, E, F) C₁₆₁₄. Calcium-titrations were performed with 2 μM CaM and 6 μM Cav1.2p in 50 mM HEPES, 100 mM KCl, 1 mM MgCl₂, 0.05 mM EGTA, 5 mM NTA, 0.1 μM XRhod5F, pH 7.4 at 22 °C. Titration curves were simulated according to Eq. (5), based on free energies of calcium binding to CaM alone (dashed lines) and to CaM:Cav1.2p complexes (solid lines) given in Table 2.

The decrease in Phe and increase in Tyr fluorescence from the N- and C-domains of CaM were monitored throughout the Ca^{2+} -titrations. For CaM alone (i.e., in the absence of a bound peptide), the Phe residues within the C-domain do not contribute to the total Phe signal. Thus, the intensity can be assigned solely to the calcium-dependent response of the N-domain of CaM [34]. Changes in the intensity of Phe fluorescence upon Ca^{2+} -binding to the N-domain and Tyr fluorescence upon Ca^{2+} -binding to the C-domain of CaM_{1–148} are shown in Figs. 7 and 8 as dashed lines. The data were fit to a model-independent two-site (Adair) function (Eq. (6)). In the absence of peptide, the free energy (ΔG_2) of Ca^{2+} binding to the N-domain of CaM_{1–148} was -12.82 ± 0.09 kcal/mol and to the C-domain of CaM_{1–148} was -15.06 ± 0.03 kcal/mol. ΔG_2 of Ca^{2+} binding to both CaM_{1–80} and CaM_{76–148} was slightly less favorable than the ΔG_2 measured for the domains of full length CaM_{1–148}. ΔG_2 of Ca^{2+} -binding to CaM_{1–80} was -12.76 ± 0.09 kcal/mol and ΔG_2 of Ca^{2+} -binding to CaM_{76–148} was -14.66 ± 0.13 kcal/mol in the absence of a peptide.

The effect of Ca_v1.2 CTT peptide binding on the Ca^{2+} binding affinity of CaM was measured in the presence of increasing molar ratios of Ca_v1.2 peptides. Ca^{2+} -titrations of CaM_{1–148} and CaM_{76–148} in the presence of A₁₅₈₈, C₁₆₁₄ and IQ₁₆₅₀ showed that the C-domain Phe signal was not silent and contributed to the Phe signal of CaM_{1–148} (see Materials and methods for the discussion). Therefore, the data for Ca^{2+} -binding to the N-domain of CaM were fit to Eq. (8c), taking into account the Phe contribution from the C-domain of CaM.

3.6. Effect of A₁₅₈₈ and C₁₆₁₄ on the Ca^{2+} -binding affinity of CaM

Addition of a 3-fold excess of A₁₅₈₈ to CaM_{1–148} increased the Ca^{2+} -binding affinity of both domains of CaM_{1–148}; however, the N-domain of CaM_{1–148} experienced a much greater increase ($\Delta\Delta G_2^{\text{app}}$ of -2.99 kcal/mol) than the C-domain ($\Delta\Delta G_2^{\text{app}}$ of -1.05 kcal/mol) (Table 2). The apparent free energy of Ca^{2+} -binding (ΔG_2^{app}) was -15.81 ± 0.05 kcal/mol for the N-domain and -16.11 ± 0.04 kcal/mol for the C-domain of full-length CaM_{1–148}. Phe residues located within the C-domain of CaM_{1–148} contributed ~32% of the overall signal change, as determined from the titrations of CaM_{76–148} in the presence of A₁₅₈₈ (see Materials and methods). Therefore, Eq. (8c) was used to determine the Ca^{2+} -binding affinity of the N-domain of CaM_{1–148} in the presence of A₁₅₈₈ (Fig. 7A). Both domains of CaM_{1–148} had a similar Ca^{2+} -binding affinity in the presence of A₁₅₈₈.

To explore the effect of A₁₅₈₈ on the Ca^{2+} -binding affinity of the domains of CaM, Ca^{2+} titrations of CaM_{1–80} and CaM_{76–148} were performed in the presence of 3-fold molar excess of A₁₅₈₈. Addition of A₁₅₈₈ increased the Ca^{2+} -binding affinity of CaM_{1–80} (Fig. 7B) by -1.55 kcal/mol and CaM_{76–148} (Fig. 7C) by -0.72 kcal/mol. The larger effect of the peptide on the Ca^{2+} binding affinity of sites I and II, whether in the N-domain of CaM_{1–148} or the isolated domain CaM_{1–80}, is also consistent with the anisotropy experiments, where the affinity of Fl-A₁₅₈₈ for CaM_{1–80} was about 6-fold more favorable than that for the C-domain CaM_{76–148}.

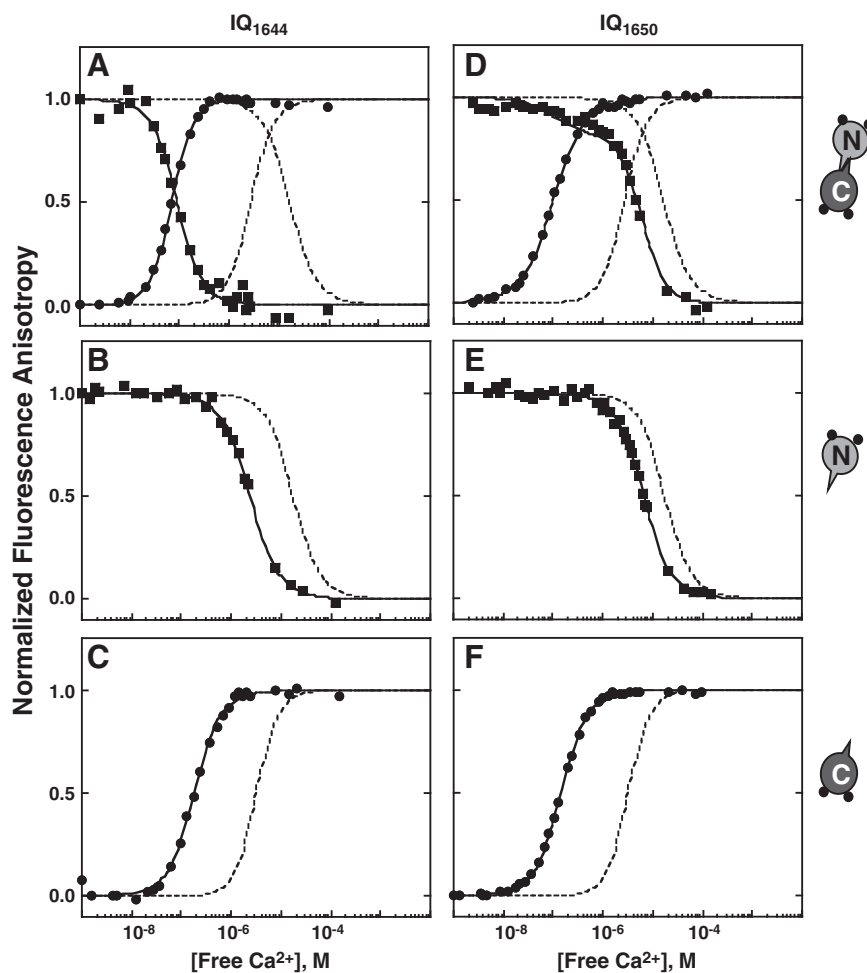


Fig. 8. Equilibrium Ca^{2+} -titrations of CaM with IQ₁₆₄₄ and IQ₁₆₅₀. Titrations of (A and D) CaM_{1–148}, (B and E) CaM_{1–80} and (C and F) CaM_{76–148} in the presence of IQ₁₆₄₄ (A, B, C) and IQ₁₆₅₀ (D, E, F). Ca^{2+} -titrations were performed with 2 μM CaM and 8 μM IQ₁₆₄₄ or 6 μM IQ₁₆₅₀ in 50 mM HEPES, 100 mM KCl, 1 mM MgCl₂, 0.05 mM EGTA, 5 mM NTA, 0.1 μM XRhod5F, pH 7.4 at 22 °C. Titration curves were simulated according to Eq. (5), based on free energies of calcium binding to CaM alone (dashed lines) and to CaM:Ca_v1.2p (solid lines) given in Table 2.

Table 2
Effect of Ca_v1.2 CTT peptides on free energies of calcium binding to CaM.

Protein	Ca _v 1.2p	ΔG_1^{app}	ΔG_2^{app}	$\Delta\Delta G_2^{\text{a,b}}$
Sites I and II				
CaM _{1–80}	– ^c	–5.92 ± 0.38	–12.76 ± 0.09	–
	1588	–7.13 ± 0.17	–14.31 ± 0.06	–1.55
	1614	–6.60 ± 0.28	–13.91 ± 0.08	–1.15
	1644	–7.48 ± 0.20	–15.25 ± 0.07	–2.49
	1650	–6.66 ± 0.22	–13.58 ± 0.15	–0.82
CaM _{1–148}	– ^c	–5.98 ± 0.02	–12.82 ± 0.09	–
	1588	–7.00 (fixed)	–15.81 ± 0.05	–2.99
	1614	–6.59 ± 0.13	–13.92 ± 0.14	–1.10
	1644	–8.47 ± 1.07	–19.19 ± 0.18	–6.37
	1650	–7.00 (fixed)	–14.06 ± 0.04	–1.24
Sites III and IV				
CaM _{76–148}	– ^c	–5.45 ± 0.51	–14.66 ± 0.13	–
	1588	–7.32 ± 0.04	–15.38 ± 0.18	–0.72
	1614	–8.25 ± 0.16	–17.61 ± 0.20	–2.95
	1644	–8.71 ± 0.20	–18.27 ± 0.07	–3.61
	1650	–8.47 ± 0.07	–18.01 ± 0.04	–3.35
CaM _{1–148}	– ^c	–6.40 ± 0.19	–15.06 ± 0.03	–
	1588	–7.00 (fixed)	–16.11 ± 0.04	–1.05
	1614	–8.94 ± 0.13	–18.00 ± 0.06	–2.94
	1644	–8.16 ± 0.35	–19.37 ± 0.06	–4.31
	1650	–9.25 ± 0.17	–18.69 ± 0.22	–3.63

^a $\Delta\Delta G_2 = \Delta G_2^{\text{app}}(\text{CaM} + \text{CaV1.2p}) - \Delta G_2^{\text{app}}(\text{CaM})$.^b kcal/mol.^c No peptide.

The presence of C₁₆₁₄ also increased the Ca²⁺-binding affinity of both domains of CaM_{1–148} (Fig. 7D). The affinity of the C-domain of CaM_{1–148} experienced a greater increase in the Ca²⁺-binding affinity than the N-domain ($\Delta\Delta G_2^{\text{app}}$ of –2.94 kcal/mol for the C-domain versus $\Delta\Delta G_2^{\text{app}}$ of –1.10 kcal/mol for the N-domain). In the presence of C₁₆₁₄, Phe residues located within the C-domain of CaM_{1–148} contributed 8% to the overall signal change. Therefore, ΔG_2^{app} of Ca²⁺-binding to the N-domain of CaM_{1–148} was calculated using Eq. (8c).

Binding of C₁₆₁₄ increased the Ca²⁺-binding affinity of both CaM_{1–80} (Fig. 7E) and CaM_{76–148} (Fig. 7F), which was similar to the increase determined for the domains of CaM_{1–148} with a higher increase in the Ca²⁺-binding affinity of CaM_{76–148} compared to CaM_{1–80} ($\Delta\Delta G_2^{\text{app}}$ of –2.95 kcal/mol for CaM_{76–148} and $\Delta\Delta G_2^{\text{app}}$ of –1.15 kcal/mol for CaM_{1–80}) (Table 2). These results contrast with a previous study [18] indicating that, while C₁₆₁₄ increased the Ca²⁺-binding affinity of the C-domain of CaM_{1–148}, there was not an effect on the N-domain. This difference in conclusions may reflect differences in discrimination possible with the methods.

3.7. Effect of IQ₁₆₄₄ and IQ₁₆₅₀ on the Ca²⁺-binding affinity of CaM

To understand how the anchoring residues surrounding the N-termina region of Ca_v1.2 CTT IQ motif affect the Ca²⁺-binding affinity of CaM, we performed Ca²⁺-titrations in the presence and absence of IQ₁₆₄₄ or IQ₁₆₅₀. The presence of IQ₁₆₄₄ did not significantly change the Phe signal of the CaM_{76–148}. Therefore, ΔG_2^{app} of Ca²⁺-binding to the N-domain of CaM_{1–148} was calculated using Eq. (2). The magnitude of increase in the Ca²⁺-binding affinity of the N-domain was greater than the increase in the C-domain in the presence of IQ₁₆₄₄ ($\Delta\Delta G_2^{\text{app}}$ of –6.37 kcal/mol for the N-domain and –4.31 kcal/mol for the C-domain) (Fig. 8A). Overall, Ca²⁺-binding affinities of both domains of CaM_{1–148} were more similar in the presence of IQ₁₆₄₄ (Fig. 8A), which agrees with previously reported results [57]. A large increase in ΔG_2^{app} of Ca²⁺-binding affinity was also seen when IQ₁₆₄₄ was bound to CaM_{1–80} (Fig. 8B) and CaM_{76–148} (Fig. 8C). The Ca²⁺-binding affinity of both CaM_{1–80} and CaM_{76–148} became more favorable ($\Delta\Delta G_2^{\text{app}}$ of –2.49 kcal/mol for CaM_{1–80} and –3.61 kcal/mol for CaM_{76–148}). The binding affinity of sites I and II in the N-domain of CaM_{1–148} increased much more than the same sites

in the N-domain alone, CaM_{1–80}, ($\Delta\Delta G_2^{\text{app}}$ of –6.37 kcal/mol for sites I and II in CaM_{1–148} compared to $\Delta\Delta G_2^{\text{app}}$ of –2.49 kcal/mol for CaM_{1–80}). This is almost 4 kcal/mol. It is clear that the C-domain of full-length CaM_{1–148} contributes to the difference in the Ca²⁺-binding affinity of CaM_{1–80} and the N-domain of full-length CaM_{1–148} upon binding to IQ₁₆₄₄. Although a change in local concentration of the N-domain of full-length CaM at the binding site may contribute, the positioning of the N-domain is also restricted once the C-domain has bound.

IQ₁₆₅₀ binding increased the Ca²⁺-binding affinity of both domains of CaM_{1–148} (Fig. 8D). There was an 18% Phe signal contribution to the overall signal change from Phe residues in the C-domain of CaM_{1–148} in the presence of IQ₁₆₅₀. Therefore, ΔG_2^{app} of Ca²⁺-binding to the N-domain of CaM_{1–148} in the presence of IQ₁₆₅₀ was calculated using Eq. (8c). The increase in the Ca²⁺-binding affinity of sites I and II of CaM_{1–148} was not as great as the increase seen in the presence of IQ₁₆₄₄ ($\Delta\Delta G_2^{\text{app}}$ of –1.10 kcal/mol and –6.37 kcal/mol, respectively). IQ₁₆₅₀ also increased the Ca²⁺-binding affinity of the C-domain of CaM_{1–148} ($\Delta\Delta G_2^{\text{app}}$ = –3.63 kcal/mol) but to a slightly lesser extent than IQ₁₆₄₄ binding ($\Delta\Delta G_2^{\text{app}}$ = –4.31 kcal/mol).

The Ca²⁺-binding affinity of CaM_{1–80} increased in the presence of IQ₁₆₅₀ ($\Delta\Delta G_2^{\text{app}}$ of –0.82 kcal/mol) but to a lower extent than in the presence of IQ₁₆₄₄ binding ($\Delta\Delta G_2^{\text{app}}$ of –2.49 kcal/mol). However, the increase in Ca²⁺-binding affinity of CaM_{76–148} upon binding to IQ₁₆₅₀ was similar to the change observed for the effect of binding IQ₁₆₄₄ ($\Delta\Delta G_2^{\text{app}}$ of –3.35 kcal/mol and –3.61 kcal/mol, respectively).

A summary plot of $\Delta\Delta G_2$ of calcium binding to sites I and II in the N-domain of CaM_{1–148} and in CaM_{1–80} and sites III and IV in the C-domain of CaM_{1–148} and in CaM_{76–148} is shown in Fig. 9. When comparing the Ca_v1.2p sequences studied, it is apparent that the N-terminal anchoring residues of IQ₁₆₄₄ play a role in producing the largest increase in the Ca²⁺-binding affinity of sites I and II in full-length CaM (dark bar in Fig. 9A). IQ₁₆₄₄ binding also increased the Ca²⁺-binding affinity of sites III and IV to the greatest extent (Fig. 9B). C₁₆₁₄ and IQ₁₆₅₀ had a much weaker effect on the Ca²⁺-binding affinity of the N-domain of CaM.

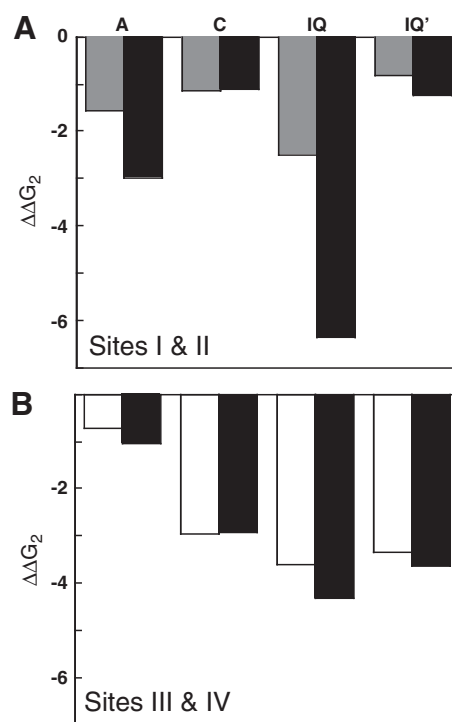


Fig. 9. Effect of Ca_v1.2 peptides on free energy ($\Delta\Delta G_2$) of Ca²⁺-binding to CaM. Comparison ($\Delta\Delta G_2$) of calcium binding to (A) sites I and II and (B) sites III and IV in CaM alone and CaM bound to a Ca_v1.2 peptide. CaM_{1–80} (gray bars), CaM_{76–148} (open bars) and N- and C-domains of CaM_{1–148} (black bars) in the presence of Ca_v1.2p.

Likewise, A₁₅₈₈ had a weak effect on the Ca²⁺-binding affinity of the C-domain of CaM.

3.8. Thermodynamic insights into structural models of the CTT

Fig. 10 summarizes the thermodynamic findings for Ca²⁺-dependent CaM interactions with sites A, C and IQ/IQ' in the CTT of Ca_v1.2. As shown in Fig. 10A, no individual site binds a single domain of apo CaM strongly; although, CaM may bind to sites in combination, while Ca²⁺ is entering the channel. CaM binds to C₁₆₁₄ and IQ₁₆₄₄ under low “resting” Ca²⁺ levels as mimicked by association measured in 146 nM free calcium (Fig. 10B). This level is sufficient to saturate the C-domain of CaM and possibly both domains depending on the specific target interaction under consideration. However, the free N-domain is not saturated with Ca²⁺ at 146 nM. At high calcium, (Ca²⁺)₄-CaM_{1–148} bound to all of the peptides with high affinity, but binding to IQ₁₆₄₄ was the most favorable. Studies of the individual domains of CaM demonstrated that A₁₅₈₈ was unusual in binding the N-domain of CaM more favorably than the C-domain.

Fig. 11 integrates the thermodynamic data for the linked binding of calcium and Ca_v1.2 peptides with recent structural studies of calcium-saturated CaM bound to long peptide encompassing the A–C–IQ sites (3G43 [24] and 3OXQ [51]). Because of the similarities between these structures, only one (3G43) is shown in Fig. 11A to represent the observation that two (Ca²⁺)₄-CaM_{1–148} molecules bridge a coiled-coil region containing sites A and C, while (Ca²⁺)₄-CaM_{1–148} engulfs each IQ motif, as had been observed previously by these groups. The sequence linking C to IQ was not ordered in either structure. On the basis of 3G43, Hamilton and coworkers proposed that there is a physiological role for a dimer of Ca_v1.2. They created a mutation

(substitution of E to P) in the QANE sequence that was designed to disrupt the coiled-coil interaction. It had a deleterious effect on the channel, which could be attributed to disruption of dimerization.

Minor and coworkers sought to find evidence of dimerization in vitro and in vivo, and concluded that while multiple CaM molecules bind the CTT, the functional form of Ca_v1.2 is a monomer [51]. Furthermore, based on sequence similarity with the voltage-gated sodium channels, and structures available for the EF-hands of Na_v1.2 [58] and Na_v1.5 [59], they proposed that site A is folded within the EF-hand of Ca_v1.2, and therefore inaccessible to CaM under normal cellular conditions (see Supp. Fig. 6, [51]). Thus, interaction of the N-domain of CaM there would be artefactual despite its high affinity.

Examining the sequences of Ca_v1.2 and Na_v1.2, we aligned ALRIKTE in Ca_v1.2 with ALRIQME in Na_v1.2. This alignment differs from the report of 3OXQ [51]. Conserved (underlined) residues are highlighted in the drawings of the structures of (i) dimeric Ca_v1.2 CTT (3G43, left side of Fig. 11A) and (ii) Na_v1.2 EF-hand (2KAV, right side of Fig. 11A). In Na_v1.2, the sequence ALRIQME is in a helix adjacent to the folded EF-hand and adopts many different positions in the 15 NMR models reported by Palmer and coworkers [58]. The ALRIKTE sequence within site “A” of Ca_v1.2 is downstream of the presumptive EF-hand motif of Ca_v1.2, and precedes the QANE sequence. In 3G43, it interacts with both the N- and C-domains of CaM.

The dimeric Ca_v1.2 structures 3G43 and 3OXQ represent a tour de force in crystallographic effort and show energetically accessible states of CaM–Ca_v1.2 complexes. It is very challenging to determine how they correlate with the biologically active states of Ca_v1.2, and to what extent other structures may also be viable and important. The extended helix formed by the alignment of the A and C sites harkens back to the first crystallographic structures of CaM itself in which a

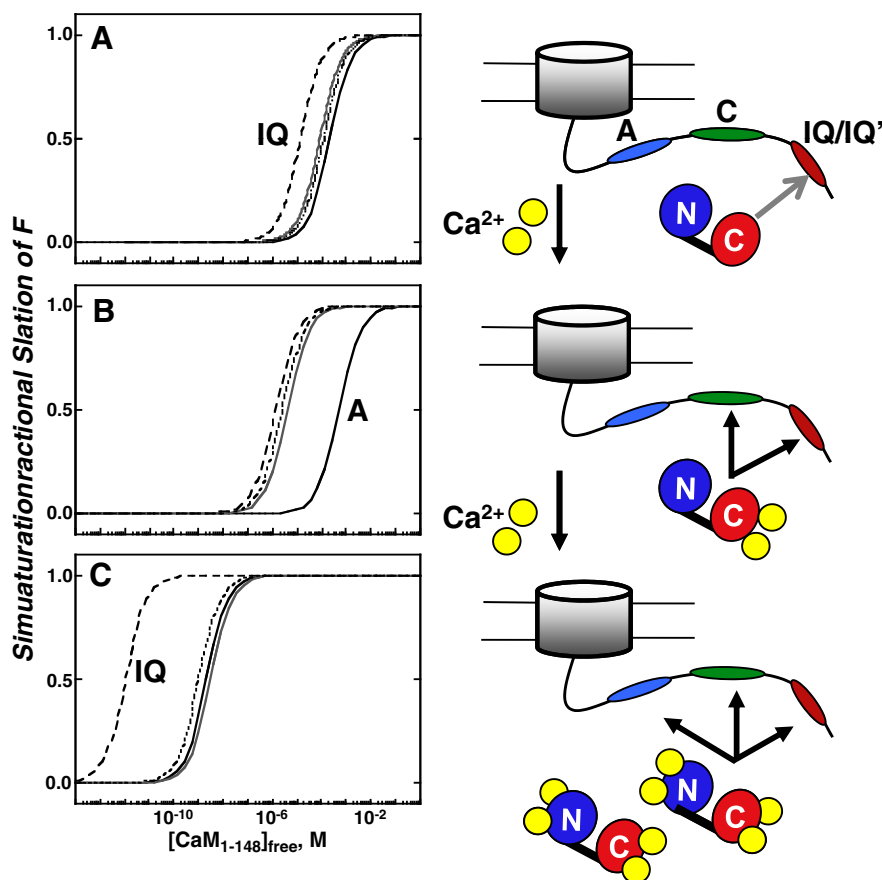


Fig. 10. Simulated titrations of CaM_{1–148} binding to Ca_v1.2p under equilibrium conditions. Apo, (B) 146 nM calcium and (C) Ca²⁺-saturated conditions. CaM_{1–148} binding to Ca_v1.2pA₁₅₈₈ (black lines), Ca_v1.2pC₁₆₁₄ (gray lines), Ca_v1.2pIQ₁₆₄₄ (dashed lines) and Ca_v1.2pIQ₁₆₅₀ (dotted lines).

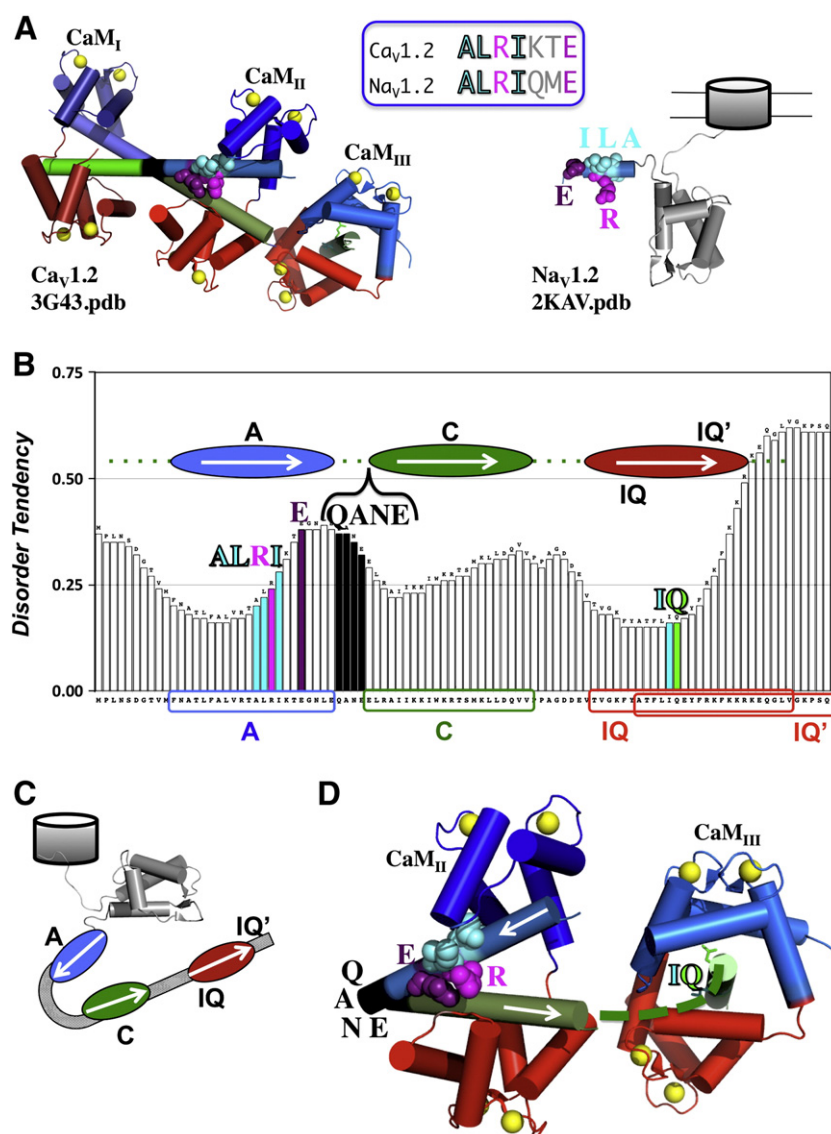


Fig. 11. Structural models for CaM binding to $\text{Ca}_v1.2$ CTT. **A.** The left side depicts 3 molecules of $(\text{Ca}^{2+})_4\text{-CaM}_{1-148}$ bound to two $\text{Ca}_v1.2$ peptides as seen in the crystallographic structure 3G43 [24]; the subscripted designation of CaM molecules follows that of the original publication. CaM_I and CaM_{II} are bound to a pair of A–C (pre-IQ) peptides that form a coiled-coil structure (indicated by two cylinders that cross at the black midpoint) denoting the sequence QANE (corresponding to residues 1610–1613 in the sequence used in Fig. 1, between “A” and “C”). For one of these peptides, an extension containing the IQ motif bound to CaM_{III} was visible orthogonal to the A–C peptide. The right side depicts 2KAV (model 6, [58]), an NMR structure of the EF-hand region of $\text{Na}_v1.2$ which has features similar to the sequence preceding the “A” site of $\text{Ca}_v1.2$. The location of a sequence (ALRIQME) found in $\text{Na}_v1.2$ is highlighted with cyan for the aliphatic groups (A, L, I), purple for E and magenta for R depicting residues that are identical in a corresponding sequence (ALRIKTE) found in the A site in $\text{Ca}_v1.2$. **B.** Disorder Tendency of A–C–IQ–IQ’ region of $\text{Ca}_v1.2$. Bar graph of predicted disorder calculated by metaPrDOS (protein disorder meta-prediction server <http://prdos.prdos.hgc.jp/meta/>) [60] for subset of $\text{Ca}_v1.2$ sequence containing the A, C, IQ and IQ’ sites. **C.** Schematic model of jointed tertiary structure for A–C–IQ region. If the sequence (residues QANE) between A_{1588} and C_{1614} participates in a turn or bend, $(\text{Ca}^{2+})_4\text{-CaM}$ binding could cause an intramolecular rearrangement bringing the A (blue oval) and C (green oval) sites together. This could bring the intrinsic EF-hand domain (gray, based on model 6 from 2KAV from $\text{Na}_v1.2$) closer to the IQ motif (red oval) of $\text{Ca}_v1.2$. **D.** Tertiary complex consistent with thermodynamic properties. A model based on the positions of CaM_{II} and CaM_{III} in the dimeric structure in 3G43 shown in panel A, and the schematic in panel C. $(\text{Ca}^{2+})_4\text{-CaM}_{II}$ brings contiguous sites A and C together after a bend occurs beginning near the terminal E1605 of the ALRIKTE sequence (color scheme matches panel A), and extending through the black region labeled QANE (terminal glutamate is E1613). Site C is connected to the IQ motif (the dashed green curve represents residues not observed in the crystallographic structure).

long helix was observed between the N- and C-domains. Later, it was recognized that the extended helix was promoted by crystallization conditions and represented a snapshot of CaM when a shorter helix “D” (the fourth helix of the N-domain) and similar helix “E” (the first helix of the C-domain) were aligned along the same axis. NMR later showed that the two domains of CaM could move freely relative to one another and that this contributed to the ability of CaM to regulate many targets. In conjunction with structural studies, thermodynamic measurements provide boundary conditions for such models and allow us to consider what the most likely, or highly populated, states of these components of the channel will be.

$\text{Ca}_v1.2$ is a modular protein that interacts with CaM in complex ways to mediate distinct biological effects. With the thought of flexible linkers and multiple conformations in mind, we used metaPrDOS (protein disorder meta-prediction server, <http://prdos.hgc.jp/meta/>) [60] to predict the disorder tendency to assess the likelihood of a flexible joint or linker between sites A and C in the A–C–IQ–IQ’ region of $\text{Ca}_v1.2$. The results are shown in Fig. 11B. The ALRI residues precede a sequence that is predicted to be disordered beginning at the terminal E (shown in purple) of ALRIKTE. Note that the sequence QANE that mediates the coiled-coil interaction shown in black in Fig. 11A is a sequence that is between the peptides we

selected to represent sites A and C. This sequence is predicted to have a disorder tendency higher than that for the initial residues of site C.

This analysis suggests that the ovals representing A, C, and IQ/IQ' may re-arrange according to the schematic "hairpin" model shown in Fig. 11C which indicates that $(\text{Ca}^{2+})_4\text{-CaM}_{1-148}$ may clasp site A (via its N-domain) and site C (via its C-domain), which would significantly change the quaternary structure of the CTT. This would be consistent with an earlier model of CaM binding to these sequences under resting calcium levels [16]. An additional CaM molecule may bind the IQ region, and also bind to locations outside the CTT where CaM has been identified to interact [12,23,61,62].

3.9. Summary

This study demonstrates that each domain of CaM plays distinct roles in binding to the 3 major sites within the $\text{Ca}_v1.2$ CTT, and that thermodynamic linkage between calcium-binding and channel-binding creates a hierarchy of states that are accessible to CaM. Ongoing studies of the interplay between energetic driving forces for structural change, as well as correlations with extra-thermodynamic information, offer much hope for dissecting the contributions of CaM interactions within the context of a whole ion channel. The ultimate goal of understanding all of the roles of CaM is yielding to new methods that allow us to monitor the roles of the N- and C-domains separately and to recombine them to determine to what extent the whole is greater than the sum of its parts.

Supplementary materials related to this article can be found online at doi:10.1016/j.bpc.2011.06.007.

Acknowledgments

The intracellular domains of ion channels are essential for regulation, but devilishly inaccessible to direct binding studies. Structural biology provides highly detailed information about individual states that are energetically accessible, but does not indicate the probability of those states. To understand competition among neighboring sites, a thermodynamic analysis allows us to assess probabilities of states of the system and ultimately connect these to biological events. In this work, we have gained inspiration and benefited from criticism offered by our colleagues participating in the annual *Gibbs Conference on Biothermodynamics* which will be held for the 25th time in 2011. Through this conference, we deepened our understanding of many areas of functional thermodynamics of biological systems, and shared ideas about how macromolecules conduct life's business. The theory of individual-site binding analysis developed with Michael Brenowitz, Donald Seneor, Francine Smith and the late Gary K. Ackers was immediately applied to studying calcium binding to the domains of CaM, which have some striking resemblances to the left and right operators of bacteriophage lambda, as well as the $\alpha - \beta$ dimers of the hemoglobin tetramer, particularly the concepts of quaternary enhancement and intra-dimer cooperativity. We benefited from the pioneering insights of Timothy Lohman and Wlodek Bujalowski on molecular binding density functions and sought their guidance regarding the nature of thermodynamic information that can be obtained when signal-to-noise or signal partitioning between sites forced some experiments to be conducted under stoichiometric or sub-stoichiometric conditions. We often consulted the monograph *Binding and Linkage* by the late Stanley Gill and Jeffries Wyman.

As we were discovering the important anti-cooperative role of the linker region of CaM, and the energetic effect it exerts to separate the calcium-binding response of the two domains, despite their structural "identity" (backbone RMSD < 1 Å), we benefited from discussions of protein folding and electrostatic forces in proteins with Nathan Baker, Douglas Barrick, D. Wayne Bolen, Trevor Creamer, Bertrand Garcia-Moreno, Michael Henzl, Vincent Hilser, Nick Pace, Rohit Pappu,

George Rose, and Jurg Rösigen. We were inspired by the elegant integration of thermodynamic theories of allostery, ionic interactions, and structural studies of Enrico Di Cera. We have discussed the hidden regulatory role of linkers in allosteric DNA-binding proteins with Dorothy Beckett, Jannette Carey, James C. Lee and Liskin Swint-Kruse, and hydrodynamic methods to delineate size and stoichiometry of regulatory complexes with Jack Correia, Jim Cole, Walter Stafford and Michael Johnson. To judge the validity of, and discriminate between, models of equilibrium ligand binding, we have depended on the nonlinear least-squares analysis software written originally by Herbert Halvorsen and Michael L. Johnson for analyzing models of cooperative oxygen binding to hemoglobin in the Ackers laboratory. We also wish to thank Mark Anderson, DJ Black, Susan Hamilton, Daniel Minor, Tony Persechini, David Yue and members of their laboratories for stimulating questions when we presented preliminary findings at the annual Biophysical Society meeting and other venues. We acknowledge support including a Postdoctoral Training Fellowship (Iowa Cardiovascular Center; T32 HL 07121-30) and NRSA Postdoctoral Fellowship (NIHF32 GM 77927) to TIAE, and NIH research grants AG0175002 (JWH) and GM57001 (MAS). We thank Laurel Coffeen Faga for assistance with figures and editing.

This manuscript is dedicated to the memories of Gary K. Ackers and Stanley J. Gill. They were founding members of the Gibbs Conference on Biothermodynamics, and generously shared their passion for rigorous scientific inquiry and analysis.

References

- [1] Y. Saimi, C. Kung, Ion Channel regulation by calmodulin binding, *FEBS Lett.* 350 (1994) 155–158.
- [2] A. Hudmon, H. Schulman, J. Kim, J.M. Maltez, R.W. Tsien, G.S. Pitt, CaMKII tethers to L-type Ca^{2+} channels, establishing a local and dedicated integrator of Ca^{2+} signals for facilitation, *J. Cell Biol.* 171 (2005) 537–547.
- [3] T.S. Lee, R. Karl, S. Moosmang, P. Lenhardt, N. Klugbauer, F. Hofmann, T. Kleppisch, A. Wellig, Calmodulin kinase II is involved in voltage-dependent facilitation of the L-type $\text{Ca}_v1.2$ calcium channel: identification of the phosphorylation sites, *J. Biol. Chem.* 281 (2006) 25560–25567.
- [4] I. Dzura, Y. Wu, R.J. Colbran, J.R. Balsar, M.E. Anderson, Calmodulin kinase determines calcium-dependent facilitation of L-type calcium channels, *Nat. Cell Biol.* 2 (2000) 173–177.
- [5] C.E. Grueter, S.A. Abiria, I. Dzura, Y. Wu, A.J. Ham, P.J. Mohler, M.E. Anderson, R.J. Colbran, L-type Ca^{2+} channel facilitation mediated by phosphorylation of the beta subunit by CaMKII, *Mol. Cell* 23 (2006) 641–650.
- [6] R.D. Zühlke, G.S. Pitt, K. Deisseroth, R.W. Tsien, H. Reuter, Calmodulin supports both inactivation and facilitation of L-type calcium channels, *Nature* 399 (1999) 159–162.
- [7] B.Z. Peterson, J.S. Lee, J.G. Mülle, Y. Wang, M. de Leon, D.T. Yue, Critical determinants of Ca^{2+} -dependent inactivation within an EF-hand motif of L-type Ca^{2+} channels, *Biophys. J.* 78 (2000) 1906–1920.
- [8] C. Romanin, R. Gamsjaeger, H. Kahr, D. Schaufler, O. Carlson, D.R. Abernethy, N.M. Soldatov, Ca^{2+} sensors of L-type Ca^{2+} channel, *FEBS Lett.* 487 (2000) 301–306.
- [9] D.B. Halling, P. Aracena-Parks, S.L. Hamilton, Regulation of voltage-gated Ca^{2+} channels by calmodulin, *Sci. STKE* 315 (2005) 1–11.
- [10] T. Cens, M. Rousset, J.P. Leyris, P. Fesquet, P. Charnet, Voltage- and calcium-dependent inactivation in high voltage-gated Ca^{2+} channels, *Prog. Biophys. Mol. Biol.* 90 (2006) 104–117.
- [11] H. Liang, C.D. DeMaria, M.G. Erickson, M.X. Mori, B.A. Alseikhan, D.T. Yue, Unified mechanisms of Ca^{2+} regulation across the Ca^{2+} channel family, *Neuron* 39 (2003) 951–960.
- [12] I.E. Dick, M.R. Tadross, H. Liang, L.H. Tay, W. Yang, D.T. Yue, A modular switch for spatial Ca^{2+} selectivity in the calmodulin regulation of Ca_v channels, *Nature* 451 (2008) 830–834.
- [13] J.L. Fallon, D.B. Halling, S.L. Hamilton, F.A. Quiocho, Structure of calmodulin bound to the hydrophobic IQ domain of the cardiac $\text{Ca}_v1.2$ calcium channel, *Structure* 13 (2005) 1881–1886.
- [14] F. van Petegem, F.C. Chatelain, D.L. Minor Jr., Insights into voltage-gated calcium channel regulation from the structure of the $\text{Ca}_v1.2$ IQ domain– Ca^{2+} /calmodulin complex, *Nat. Struct. Mol. Biol.* 12 (2005) 1108–1115.
- [15] V. Sobolev, A. Sorokine, J. Prilusky, E.E. Abola, M. Edelman, Automated analysis of interatomic contacts in proteins, *Bioinformatics* 15 (1999) 327–332.
- [16] G.S. Pitt, R.D. Zühlke, A. Hudmon, H. Schulman, H. Reuter, R.W. Tsien, Molecular basis of calmodulin tethering and Ca^{2+} -dependent inactivation of L-type Ca^{2+} channels, *J. Biol. Chem.* 276 (2001) 30794–30802.
- [17] J. Mouton, A. Feltz, Y. Maulet, Interactions of calmodulin with two peptides derived from the C-terminal cytoplasmic domain of the $\text{Ca}_v1.2$ Ca^{2+} channel provide evidence for a molecular switch involved in Ca^{2+} -induced inactivation, *J. Biol. Chem.* 276 (2001) 22359–22367.

- [18] W. Tang, D.B. Halling, D.J. Black, P. Pate, J.Z. Zhang, S. Pedersen, R.A. Altschuld, S.L. Hamilton, Apocalmodulin and Ca^{2+} calmodulin-binding sites on the $\text{Ca}_v1.2$ channel, *Biophys. J.* 85 (2003) 1538–1547.
- [19] R.D. Zuhlke, G.S. Pitt, R.W. Tsien, H. Reuter, Ca^{2+} -sensitive inactivation and facilitation of L-type Ca^{2+} channels both depend on specific amino acid residues in a consensus calmodulin-binding motif in the $\alpha_1\text{C}$ subunit, *J. Biol. Chem.* 275 (2000) 21121–21129.
- [20] B.Z. Peterson, C.D. DeMaria, D.T. Yue, Calmodulin is the Ca^{2+} sensor for Ca^{2+} -dependent inactivation of L-type calcium channels, *Neuron* 22 (1999) 549–558.
- [21] M.G. Erickson, H. Liang, M.X. Mori, D.T. Yue, FRET two-hybrid mapping reveals function and location of L-Type Ca^{2+} channel CaM preassociation, *Neuron* 39 (2003) 97–107.
- [22] L.Y. Lian, D. Myatt, A. Kitmitto, Apo calmodulin binding to the L-type voltage-gated calcium channel $\text{Ca}_v1.2$ IQ peptide, *Biochem. Biophys. Res. Commun.* 353 (2007) 565–570.
- [23] J. Kim, S. Ghosh, D.A. Nunziato, G.S. Pitt, Identification of the components controlling inactivation of voltage-gated Ca^{2+} channels, *Neuron* 41 (2004) 745–754.
- [24] J.L. Fallon, M.R. Baker, L. Xiong, R.E. Loy, G. Yang, R.T. Dirksen, S.L. Hamilton, F.A. Quiocho, Crystal structure of dimeric cardiac L-type calcium channel regulatory domains bridged by Ca^{2+} calmodulins, *Proc. Natl. Acad. Sci. U.S.A.* 106 (2009) 5135–5140.
- [25] E.Y. Kim, C.H. Rumpf, F. Van Petegem, R.J. Arant, F. Findeisen, E.S. Cooley, E.Y. Isacoff, D.L. Minor Jr., Multiple C-terminal tail $\text{Ca}(2+)/\text{CaMs}$ regulate $\text{Ca}(V)1.2$ function but do not mediate channel dimerization, *EMBO J.* 29 (2010) 3924–3938.
- [26] B.R. Sorensen, L.A. Faga, R. Hultman, M.A. Shea, Interdomain linker increases thermostability and decreases calcium affinity of calmodulin N-domain, *Biochemistry* 41 (2002) 15–20.
- [27] B.R. Sorensen, M.A. Shea, Interactions between domains of apo calmodulin alter calcium binding and stability, *Biochemistry* 37 (1998) 4244–4253.
- [28] S. Pedigo, M.A. Shea, Quantitative endoprotease GluC footprinting of cooperative Ca^{2+} binding to calmodulin: proteolytic susceptibility of E31 and E87 indicates interdomain interactions, *Biochemistry* 34 (1995) 1179–1196.
- [29] J.A. Putkey, G.R. Slaughter, A.R. Means, Bacterial expression and characterization of proteins derived from the chicken calmodulin cDNA and a calmodulin processed gene, *J. Biol. Chem.* 260 (1985) 4704–4712.
- [30] G.H. Beaven, E.R. Holiday, Ultraviolet absorption spectra of proteins and amino acids, *Adv. Protein Chem.* 7 (1952) 319–386.
- [31] M.L. Johnson, S.G. Frasier, Nonlinear least-squares analysis, *Methods Enzymol.* 117 (1985) 301–342.
- [32] B.A. Johnson, R.A. Blevins, NMR view: a computer program for the visualization and analysis of NMR data, *J. Biomol. NMR* 4 (1994) 603–614.
- [33] W.S. VanScyoc, M.A. Shea, Phenylalanine fluorescence studies of calcium binding to N-Domain fragments of *Paramecium* calmodulin mutants show increased calcium affinity correlates with increased disorder, *Protein Sci.* 10 (2001) 1758–1768.
- [34] W.S. VanScyoc, B.R. Sorensen, E. Rusinova, W.R. Laws, J.B. Ross, M.A. Shea, Calcium binding to calmodulin mutants monitored by domain-specific intrinsic phenylalanine and tyrosine fluorescence, *Biophys. J.* 83 (2002) 2767–2780.
- [35] A.R. Rhoads, F. Friedberg, Sequence motifs for calmodulin recognition, *FASEB J.* 11 (1997) 331–340.
- [36] A. Houdusse, J.F. Gaucher, E. Kremntsova, S. Mui, K.M. Trybus, C. Cohen, Crystal structure of apo-calmodulin bound to the first two IQ motifs of myosin V reveals essential recognition features, *Proc. Natl. Acad. Sci. U.S.A.* 103 (2006) 19326–19331.
- [37] Y. Cui, J. Wen, K.H. Sze, D. Man, D. Lin, M. Liu, G. Zhu, Interaction between calcium-free calmodulin and IQ motif of neurogranin studied by nuclear magnetic resonance spectroscopy, *Anal. Biochem.* 315 (2003) 175–182.
- [38] M.D. Feldkamp, L. Yu, M.A. Shea, Structural and energetic determinants of apo calmodulin binding to the IQ motif of the $\text{Na}_v1.2$ voltage-dependent sodium channel, *Structure* 19 (2011) 733–747.
- [39] B. Chagot, W.J. Chazin, Solution NMR structure of apo-calmodulin in complex with the IQ motif of human cardiac sodium channel $\text{Na}_v1.5$, *J. Mol. Biol.* 406 (2011) 106–119.
- [40] J. Ohrtman, B. Ritter, A. Polster, K.G. Beam, S. Papadopoulos, Sequence differences in the IQ motifs of $\text{Ca}_v1.1$ and $\text{Ca}_v1.2$ strongly impact calmodulin binding and calcium-dependent inactivation, *J. Biol. Chem.* 283 (2008) 29301–29311.
- [41] M.X. Mori, C.W. Vander Kooij, D.J. Leahy, D.T. Yue, Crystal structure of the Ca_v2 IQ domain in complex with Ca^{2+} /calmodulin: high-resolution mechanistic implications for channel regulation by Ca^{2+} , *Structure* 16 (2008) 607–620.
- [42] E.Y. Kim, C.H. Rumpf, Y. Fujiwara, E.S. Cooley, F. Van Petegem, D.L. Minor Jr., Structures of Ca_v2 Ca^{2+} /CaM–IQ domain complexes reveal binding modes that underlie calcium-dependent inactivation and facilitation, *Structure* 16 (2008) 1455–1467.
- [43] H. Koide, T. Kinoshita, Y. Tanaka, S. Tanaka, N. Nagura, G. Meyer zu Horste, A. Miyagi, T. Ando, Identification of the single specific IQ motif of myosin V from which calmodulin dissociates in the presence of Ca^{2+} , *Biochemistry* 45 (2006) 11598–11604.
- [44] K.M. Trybus, M.I. Gushchin, H. Lui, L. Hazelwood, E.B. Kremntsova, N. Volkmann, D. Hanein, Effect of calcium on calmodulin bound to the IQ motifs of myosin V, *J. Biol. Chem.* 282 (2007) 23316–23325.
- [45] A. Forest, M.T. Swulius, J.K. Tse, J.M. Bradshaw, T. Gaertner, M.N. Waxham, Role of the N- and C-lobes of calmodulin in the activation of $\text{Ca}(2+)/\text{calmodulin}$ -dependent protein kinase II, *Biochemistry* (2008) 10587–10599.
- [46] S.E. O'Donnell, L. Yu, C.A. Fowler, M.A. Shea, Recognition of beta-calcalneurin by the domains of calmodulin: thermodynamic and structural evidence for distinct roles, *Proteins* 79 (2011) 765–786.
- [47] W.H. duBell, S.R. Houser, A comparison of cytosolic free Ca^{2+} in resting feline and rat ventricular myocytes, *Cell Calcium* 8 (1987) 259–268.
- [48] S.S. Sheu, V.K. Sharma, S.P. Banerjee, Measurement of cytosolic free calcium concentration in isolated rat ventricular myocytes with quin 2, *Circ. Res.* 55 (1984) 830–834.
- [49] D.B. Halling, D.K. Georgiou, D.J. Black, G. Yang, J.L. Fallon, F.A. Quiocho, S.E. Pedersen, S.L. Hamilton, Determinants in Ca_v1 channels that regulate the Ca^{2+} sensitivity of bound calmodulin, *J. Biol. Chem.* 284 (2009) 20041–20051.
- [50] M.X. Mori, M.G. Erickson, D.T. Yue, Functional stoichiometry and local enrichment of calmodulin interacting with Ca^{2+} channels, *Science* 304 (2004) 432–435.
- [51] E.Y. Kim, C.H. Rumpf, F. Van Petegem, R.J. Arant, F. Findeisen, E.S. Cooley, E.Y. Isacoff, D.L. Minor Jr., Multiple C-terminal tail Ca^{2+} /CaMs regulate $\text{Ca}(V)1.2$ function but do not mediate channel dimerization, *EMBO J.* 29 (2010) 3924–3938.
- [52] O.B. Peersen, T.S. Madsen, J.J. Falke, Intermolecular tuning of calmodulin by target peptides and proteins: differential effects on Ca^{2+} binding and implications for kinase activation, *Protein Sci.* 6 (1997) 794–807.
- [53] B.B. Olwin, A.M. Edelman, E.G. Krebs, D.R. Storm, Quantitation of energy coupling between Ca^{2+} , calmodulin, skeletal muscle myosin light chain kinase, and kinase substrates, *J. Biol. Chem.* 259 (1984) 10949–10955.
- [54] B.B. Olwin, D.R. Storm, Calcium binding to complexes of calmodulin and calmodulin binding proteins, *Biochemistry* 24 (1985) 8081–8086.
- [55] J. Kim, S. Ghosh, H. Liu, M. Tateyama, R.S. Kass, G.S. Pitt, Calmodulin mediates Ca^{2+} sensitivity of sodium channels, *J. Biol. Chem.* 279 (2004) 45004–45012.
- [56] N.T. Theoharis, B.R. Sorensen, J. Theisen-Toupal, M.A. Shea, The neuronal voltage-dependent sodium channel type II IQ motif lowers the calcium affinity of the C-domain of calmodulin, *Biochemistry* 47 (2008) 112–123.
- [57] D.J. Black, D.B. Halling, D.V. Mandich, S. Pedersen, R.A. Altschuld, S.L. Hamilton, Calmodulin interactions with IQ peptides from voltage dependent calcium channels, *Am. J. Physiol. Cell Physiol.* 288 (2005) C669–C676.
- [58] V.Z. Miloshev, J.A. Levine, M.A. Arbing, J.F. Hunt, G.S. Pitt, A.G. Palmer III, Solution structure of the $\text{Na}_v1.2$ -terminal EF-hand domain, *J. Biol. Chem.* 284 (2009) 6446–6454.
- [59] B. Chagot, F. Potet, J.R. Balsler, W.J. Chazin, Solution NMR structure of the C-terminal EF-hand domain of human cardiac sodium channel $\text{Na}_v1.5$, *J. Biol. Chem.* 284 (2009) 6436–6445.
- [60] T. Ishida, K. Kinoshita, Prediction of disordered regions in proteins based on the meta approach, *Bioinformatics* 24 (2008) 1344–1348.
- [61] R. Zhang, I. Dzura, C.E. Grueter, W. Thiel, R.J. Colbran, M.E. Anderson, A dynamic alpha-beta inter-subunit agonist signaling complex is a novel feedback mechanism for regulating L-type Ca^{2+} channel opening, *FASEB J.* (2005) 1573–1575.
- [62] D.T. Yue, Calmodulation of voltage-gated calcium channels: frontiers of biological impact and mechanistic elegance, *Biophys. J.* 100 (2011) 7a.
- [63] P. Pate, J. Mochca-Morales, Y. Wu, J.-Z. Zhang, G.G. Rodney, I.I. Serysheva, I.I. Serysheva, B.Y. Williams, M.E. Anderson, S.L. Hamilton, Determinants for calmodulin binding on voltage-dependent Ca^{2+} channels, *J. Biol. Chem.* 275 (2000) 39786–39792.